Universidade do Minho
Escola de Ciências

Artem Drogalin

Desing and synthesis of swainsonine analogs from 2,4-benzilidene D-erythrose, assisted by theoretical studies.

março de 2019

Desing and synthesis of swainsonine analogues from 2,4-benzilidene D-erythrose, assisted by theoretical studies.

Artem Drogalin

UMinho | 2019

Universidade do Minho
Escola de Ciências

Artem Drogalin

Design and synthesis of swainsonine analogs from 2,4-benzilidene D-erythrose, assisted by theoretical studies.

Dissertação de Mestrado

Mestrado em Química Medicinal

Trabalho efetuado sob a orientação de:
Professora Doutora Maria José da Chão Alves
Doutora Tarsila Gabriel Castro

Outobro de 2019

AGRADECIMENTOS

Em primeiro lugar agradeço a minha família pelo apoio incondicional e forca que em muito contribuíram para o sucesso na minha vida académica.

Agradeço minha orientadora da tese Maria José Alves pela paciência, estímulo e os conselhos sábios que me orientaram na elaboração deste trabalho e investimento no meu profissionalismo.

Também agradeço a minha co-orientadora Tarsila Gabriela Casto por abrir área nova da química para mim, pela paciência ao meu pessimismo e pela motivação dada ao longo do trabalho.

Agradeço meu melhor amigo David S. Freitas por dicas dadas que em maioria parte funcionam bem, pela suporte e motivação em momentos difíceis.

Agradeço à Cristina Sousa por ajuda na integração no laboratório e ensino boas praticas laboratoriais na investigação.

Agradeço também aos meus colegas de Mestrado, António Lavoisier, Joana Santos, Catarina Ribeiro, Luis Carvalho, Sofia Teixeira pela companhia e disponibilidade sempre demonstrada ao longo deste percurso.

À equipa docente que deram boas aulas que contribuíram para meu crescimento pessoal e profissional.

À Dr.ª Elisa Pinto e à Dr.ª Vânia Azevedo pelo profissionalismo demonstrado na realização dos espectros de Ressonância Magnética Nuclear.

Agradeço ao resto pessoal quem contribuíram para este trabalho e que não foram referidas anteriormente, por esquecimento e stress ao longo desta época escrita de tese. Obrigado a todos.

STATEMENT OF INTEGRITY

I hereby declare having conducted this academic work with integrity. I confirm that I have not used plagiarism or any form of undue use of information or falsification of results along the process leading to its elaboration.

I further declare that I have fully acknowledged the Code of Ethical Conduct of the University of Minho.

Abstract

The development of novel molecules with biological activity is always a trend topic in chemistry, as are the development of new synthetic pathways for their synthesis. In this work functionalized hehaxydropyrroloquinolines-2,3-diol were synthetized by aminocyclization of substituted tetrahydroquinolines. Tetrahydroquinolines were obtained in two steps from protected D-erythrose and anilines: 1) condensation of aldehyde and anilines, 2) inverse electron-demand Diels-Alder cycloaddition with *N*-vinylpyrrolidone in presence Lewis acid as catalyst, (Povarov's reaction). The effect of differently *m*-substituted anilines was evaluated in terms of *regio*-selectivity of reactions. Different catalysts were also tested. In parallel to the synthetic work, were conducted theoretical studies using diverse molecular modelling techniques, namely: protein structure prediction of human Golgi α-mannosidase II and lysosomal α-mannosidase; docking studies of novel compounds against these target enzymes, and molecular dynamics simulations of inhibitor-enzyme complexes.

From a synthetic point of view, four new compounds were synthetized with moderate yields. Significant progresses have been achieved within this work to give a picture of the methodological possibilities used.

Computational results did not include the four compounds obtained in the experiment section, otherwise suggest two new hits for synthesis and biological tests.

It must be recognized that further studies combining experimental, theoretical and biological studies will led to a solution to the problem in test with a full comprehension of the systems under study.

Key words: asymmetric synthesis, docking studies, D-erythrose, hehaxydropyrroloquinoline, molecular dynamic simulations.

Resumo

O desenvolvimento de novas moléculas com atividade biológica, bem como o desenvolvimento de novas metodologias para sua síntese são tópicos importantes em química. Neste trabalho, as hexahidropirroloquinolinas-2,3-diol funcionalizadas foram sintetizadas por aminociclização de tetrahidroquinolinas substituídas. As tetra-hidroquinolinas foram obtidas em duas etapas a partir da D-eritrose protegida e anilinas: 1) condensação de aldeído e anilinas, 2) cicloadição de Diels-Alder de polaridade inversa com *N*-vinilpirrolidona na presença de ácido Lewis como catalisador (reação de Povarov). O efeito dos grupos substituintes em *meta* em anilinas foi avaliado em termos de *regio*-seletividade de cicloadição. Diferentes catalisadores também foram testados. Paralelamente ao trabalho sintético, foram feitos estudos teóricos utilizando diversas técnicas de modelação molecular, tais como: previsão da estrutura da Golgi α-manosidase II humana e α-manosidase lisossomal humana; estudos de *docking* de novos compostos nessas enzimas e simulações de dinâmica molecular de complexos inibidor-enzima.

Do ponto de vista sintético, foram sintetizados quatro novos compostos com rendimentos moderados. Foram alcançados significativos progressos que permitem entender as possibilidades do método experimental.

Os resultados computacionais não incluíram os quatro compostos obtidos na seção experimental; mas sugerem dois novos *hits* para síntese e testes biológicos.

A persecução de estudos posteriores combinando síntese, estudos teóricos e biológicos irão conduzir a uma solução para o problema em análise e melhor compreensão dos sistemas em estudo.

Palavras chave: dinâmica molecular, D-eritrose, estudos de *docking*, hehaxidropirroloquinolina, síntese assimétrica.

Preamble

This thesis is composed by four chapters:

Chapter I

In this chapter, a mini-review of what is known about swainsonine: small history of discovery, biological activity, and substituted analogue synthetic pathways in last 15 years.

Chapter II

This chapter describe theoretical work that was done, to find compounds for future synthesis and orient ways for rational design new hexahydropyrroloquinolines. The methods used in this part were: homology modeling of new human models Golgi α-mannosidase II and lysosomal α-mannosidase enzymes; docking studies; molecular dynamics.

Chapter III

This chapter describe methodology for synthesis new tetrahydroquinolines and hexahydropyrroloquinolines, using *m*-substituted anilines and protected D-erythrose as starting material.

Chapter IV

General conclusion of this work.

The first three chapters are organized as scientific articles.

Abbreviation List

ACN	Acetonitrile
B3LYP	Becke, 3-parameter, Lee–Yang–Parr function
Boc	*tert*-Butyloxycarbonyl
Bz	Benzoate
Cbz	Benzyl chloroformate
DCM	Dichloromethane
DFT	Density functional theory
DIBAL-H	Diisobutylaluminium hydride
DMP	Dess-Martin periodinane
EDG	Electron donating group
eq.	Equivalent
EWG	Electron withdrawing group
FF	Force field
FTIR	Fourier transform infrared
GMII	Golgi α-mannosidase II
hGMII	Human model Golgi α-mannosidase II
HHPQ	Hexahydropyrroloquinoline
hLM	Human model lysosomal α-mannosidase
LM	Lysosomal α-mannosidase
MD	Molecular dynamics
MM	Molecular modelling
NMMO	*N*-Methylmorpholine *N*-oxide
NMR	Nuclear magnitic ressonance
PSP	Protein Structure Prediction
RMSD	Root mean square deviation
RMSF	Root mean square fluctuation
swa	Swainsonine
TBDPS	*tert*-Butyldiphenylsilyl
TBS	*tert*-butyldimethylsilyl
TEA	Trimethylamine
TFA	Trifluoracetic acid
THF	Tetrahydrofuran
THQ	Tetrahydroquinoline
TIPS	Triisopropylsilyl
TMS	Trimethylsilyl
Tr	Trityl
η	Yeild

Index

Chapter I: Introduction

“What we do now, echoes in eternity”

Marcus Aurelius

1.1 Introduction.

Swainsonine, also known as tridolgosir, is an indolizidine alkaloid, with significant physiological activity, as potent inhibitor of α-mannosidase I and II. It is present in Nature in huge number of plants and fungi. Consumption of these plants by grazing animals, leads to a chronic wasting disease characterized by weight loss, depression, altered behavior, decreased libido, infertility, and death, have been causing enormous economic losses in livestock industries, particularly in North America.

1.1.1 History

Swainsonine (indolizidine-1,2,8-triol), **1** was firstly isolated in 1973 from *Rhizoctonia leguminicola* [1], but the structure attribution was wrong [2]. Colegate *et al*. in 1979 [3] isolated and right characterized swainsonine from *Swainsona canescens*. The principal interest for plants of *Swainsone* is due to the significant cattle, sheep and horses losses. After this discover, biological activity studies of this compound immediately started. It became clear that the inhibition of two α-mannosidase enzymes was the death cause of the animals [4]. The acid enzyme, known as lysosomal, and the neutral, known as Golgi α-mannosidases were inhibited *in vitro*, and the mostly affected α-mannosidase *in vivo* is the lysosomal [5]. The major physiological problem is connected with lysosomal storage diseases. Future works aimed to study this compound as anti-tumor agent, develop synthetic methods for swainsonine, and find analogues with lower toxicity.

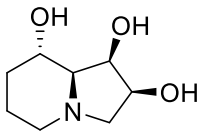

Fig. 1 Swainsonine (**1)**

1.1.2 The natural abundance of swainsonine

Principal source of swainsonine was found on rangelands in the United States in *Astragalus* and *Oxytropis* plant species. **(Img. 1)** Actually, 24 species of plant containing swainsonine compound have been recognized. The common term used for these species is locoweed plant. Locoweed poising firstly was reported in 1873, the symptomology appeared after several week of locoweed ingestion, begins with depression, dull-appearing eyes, and incoordination progressing to uncharacteristic behavior including aggression, staggering, and solitary behavior, along with wasting, and ending in death if continued consumption is allowed [6].

Img. 1 *Oxytropis sericea* [7] and *Astragalus dasyantha* [8]

As said before firstly swainsonine was isolated and characterized from *Swainsona canescens* in 1979 and the soon in 1982 the *N*-oxide form was isolated from *Astragalus lentiginosus* [9]. Most recent work showed that an endophyte fungal *Embellisia* species, isolated from *Astragalus* and *Oxytropis* species is able to synthesize toxic amounts of swainsonine [10]. This fact raises the question: "Is the swainsonine biosynthesed by the endophyte fungal colonies or by the plants themselves?"

1.1.3 Applications of swainsonine

In the next decades after swainsonine discover, biological evaluations studies start in order to find possible applications for this molecule. The alkaloid was found to inhibit lysosomal α-mannosidase and Golgi α-mannosidase II, preventing hydrolysis of mannose-rich oligosaccharides in cells and its accumulation. As a result a cell dysfunction would occur with consequent apoptosis. Potential applications of swainsonine as anti-tumor agent was deduced.

In early twenty one century several authors confirmed the inhibitory and antimetastatic effect of swainsonine in human tumors, namely hepatoma, breast and gastric carcinoma,

spongioblastoma and pate malignant tumors [11–13]. The evidences are that swainsonine is a potent anticancer agent. However, a phase II of clinical trial of hydrochloride salt of swainsonine in 17 patients with locally advanced or metastatic renal cell carcinoma show no evidence as anti-tumor activity [14]. Has been shown that swainsonine is able to inhibit tumor grow in immunodeficient mice with sarcoma in ascites form, as also was able to stop metastasis in lungs of immunodeficient mice with melanoma. In both cases the animals recovered immune responses [15].

1.2 Synthetic approaches of swainsonine

Synthetic works were started as soon as a high biological activity was found for swainsonine, with several potential fields of application. S. G. Pyne published in 2004 [16] the last review work on this topic. This section intends to revise the literature on the syntheses of D- and L-swainsonine after January 2004 till the present. Many syntheses have been developed in these last fifteen years, even after being known that pure swainsonine suffers from many side effects detected along the biological studies as referred before [17]. In what substituted swainsonine concerns only four syntheses have been registered of differently substituted swainsonine. Several of those compounds have been tested against α-mannosidase/ α-rhamnosidase and found to be more active than swainsonine itself. Developments in this field are so important from the synthetic point of view and mostly from the biological efficiency and selectivity. Computational technologies can also be useful tools to speed up an assertive solution. Evolutions of algorithms and calculation's speed increase every year, with rising concordance with experimental results. Docking screening of compounds and molecular dynamic simulations are an open source for new solutions.

This review intends to help in the future to use several swainsonine precursors as starting points to introduce substituents in swainsonine. The work is organized by common precursors systematized in three main groups (one of which is divided in two): **1i)** 8-oxy-hexahydroindolizine, and **2i)** 8-oxy-tetrahydroindolizin-5-one, **ii)** *N*-protected-3-oxy-2-substituted-piperidine, **iii)** 2-substituted-pyrrolidine-3,4-protected-diol (**Fig. 2**).

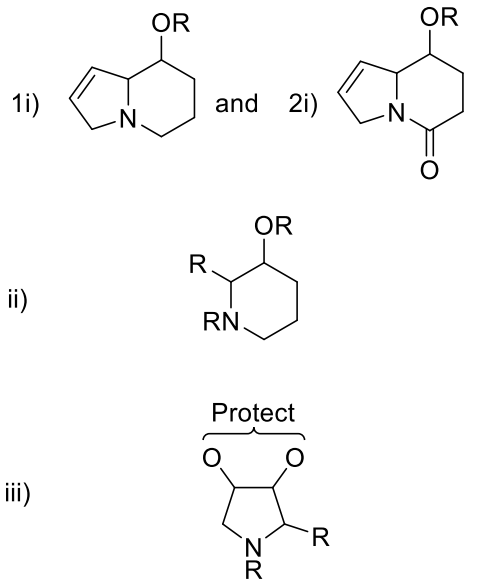

Fig. 2 The principal synthons

1.2.1 The synthesis swainsonine precursor: 8-oxy-hexahydroindolizine **1i)**

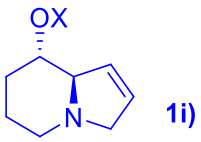

Fig. 3. 8-oxy-hexahydroindolizine precursor

In 2005 J. Ceccon *et al.* [18] propose a total synthesis of swainsonine from **1i)** intermediate (**Scheme 1**). 1,4-Pentadianol was converted into enol ether **2** and this was subjected to asymmetric [2+2] cycloaddition with dichloroketene giving dichlorocylobutanone (**3**). Chemical transformation of **3** into γ-lactam (**4**) include a Beckmann ring expansion using Tamura's reagent *O*-(mesitylsulfonyl)hydroxylamine (MSH) and a dechlorination in 12% overall yield. Allylic oxidation under Sharpless conditions (SeO_2, *t*-BuOOH, $ClCH_2CH_2Cl$, reflux) generates **5** in 56% yield. In the next the hydroxyl group was protected with triisopropylsilyl (TIPS), and the lactam was *N*-alkylated with allyl bromide giving **6**. Under Grubbs 2nd generation catalyst occurs a metasthesis process giving a bicyclic **7**. After three steps: i) hydrogenation of double bond; ii) ether cleavage under TFA; iii) amide reduction and iv) dehydration gave **1i)**.

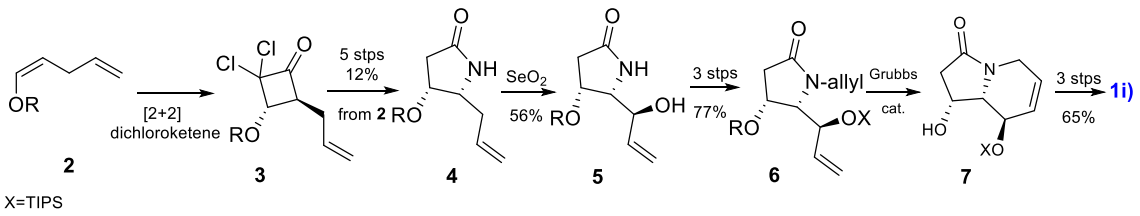

Scheme 1. J. Ceccon *et al.* synthesis

S. H. Kwon *et al.* [19] in 2007 published another method for synthesis of **1i)** (**Scheme 2**) this involves iodocyclization of the *Z*-alkene **8** using (*R*,*R*)-salen–Cr(III)Cl complex (**13**) to afford azido tetrahydrofuran **9** in 86% yield, and 90% *ee*. The azide was reducted providing an intramolecular cyclization, and the formed secondary amine was protected with *tert*-butyloxycarbonyl (Boc) group (**10**). Several transformations were then done in sequence: 1) oxidation of α-carbon of pyrrolidine with sodium periodate catalyzed by $RuCl_3$; 2) opening of the THF ring under TMSI in the presence of BF_3.ether, followed hydroxyl protection, and Boc removal to get the rearrangement to indolizidinone **11**; 3) phenylselenylation of amide α-carbon to give **12**; 4) reduction of the carbonyl with $AlLiH_4$ in the presence of $AlCl_3$, followed by an oxidative elimination of the selenium group with sodium periodate to afford **1i)**.

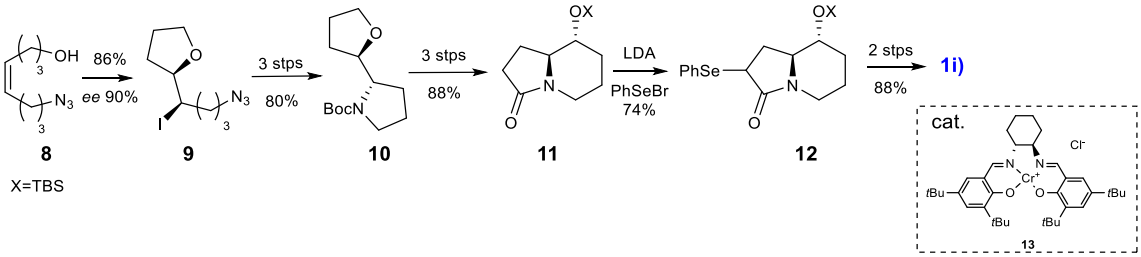

Scheme 2. S. H. Kwon *et al.* synthesis

An interesting publication of W. Bates and R. Dewey published in 2009 [20] includes a gold catalyzed reaction to achieve the six-membered ring of the indolizidine **1i)** (**Scheme 3**). Starting from THF was obtained **14**, as a racemate in a five steps synthesis with 57% overall yield. The deracemization was processed by an oxidation-reduction sequence using Corey-Bakshi-Shibata (CBS) catalyst to afford *R* isomer (**14**) in 67% yield, and *ee* 99%. The scale-up of the reaction induces a yield decreasing with formation of several byproducts. In the next step, the azide was reduced to amine, and then protected with Boc. The hydroxyl group was also protected with *tert*-butyldimethylsilyl (TBS). At last the alkyne group was subjected to homologation into the allene **15**, by Searles-Crabbe procedure. Compound **15** was cyclized into piperidine **16** under $AuCl_3$ to give a single diastereoisomer in 99% yield. Deprotection of the amine with trifluoracetic acid (TFA)

followed by alkylation with allyl carbamate (alloc) furnished the substrate for the metathesis reaction that followed, under 2nd generation Grubbs catalyst. A first alkylation attempt with allyl bromide gave only modest yield.

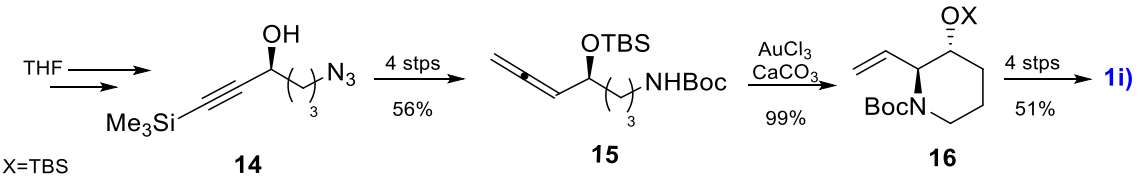

Scheme 3. W. Bates and R. Dewey synthesis

G. Archibald *et al*. in 2012 published [21] the synthesis of swainsonine from nitrone **17**, previously obtained by the same group from L-glutamate-derived hydroxy protected diester (**Scheme 4**). First lithium acetylide was added to nitrone **17**. According to the authors the stereoselectivity of the nucleophilic addition is due to an axial preference of the C-O bond in nitrone which maximize the overlapping π* (nitrone) - σ* (C-O) as the proposal of **fig. 4**. A Lindlar reduction of triple bond affords **18.**

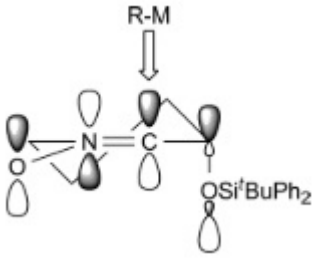

Fig. 4 Proposed stereoselectivity mechanism of nucleophilic addition to nitrone **18**

Compound **18** was further cyclized by Mitsunobu reaction using di-(4-chlorobenzyl)azodicarboxylate (DCAD), as an alternative for diethyl azodicarboxylate (DEAD) to give **1i)** in 89% yield. In the same paper vinylmagnesium bromide and allylmagnesium bromide were also efficiently added to nitrone in the presence of indium metal in 79% and 91% respectively, to give **16** *N*-deprotected type compounds. The obtained compound can also be *N*-alkylated and cyclized under Grubbs catalyst to afford **1i)**.

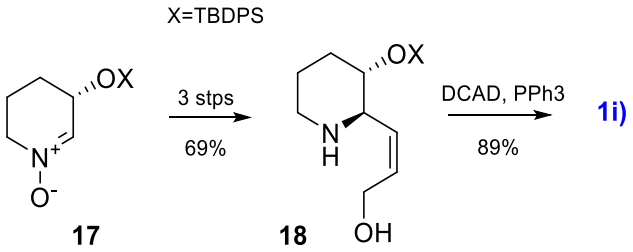

Scheme 4. G. Archibald *et al.* synthesis

The most recent literature [22] for the synthesis of swainsonine precursor **1i)** starts from achiral 5-chloropental. Chlorination of the enol ether α-carbon occurs in the presence of the organocatalyst **22** to give product **19** with 75% yield, *ee* 82%. Treatment of **19** with lithium anion of propargylamine afforded **20**. The adduct was subjected to Lindlar reduction to give the *Z* alkene. In an acid, and base sequence treatment was obtained compound **1i)** through dihydropyrrole intermediate **21**. At last, the hydroxyl group was protected with TBS.

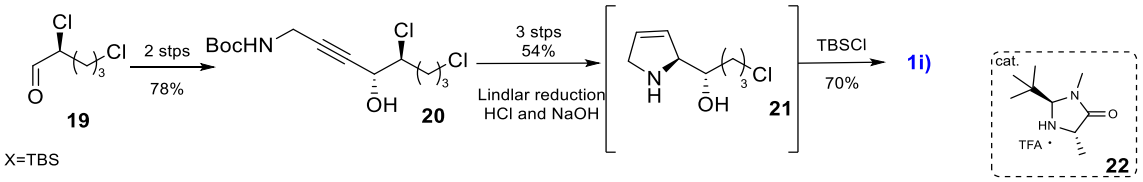

Scheme 5. V. Dhad *et al.* synthesis

1.2.2 Synthesis of swainsonine precursor: 8-oxy-tetrahydroindolizin-5-one **2i)**

Total synthesis of the swainsonine from **2i)** intermediate was reported by S. Chooprayoon and co-workers [23] in 2011 (**Scheme 6**), as the chirality source was used commercially available L-glutamic acid (**23**). To transform staring material to imide **24**, the carboxylic group was amidated by *via* transformation of this group acyl chloride and fallowed amination with 3-phenylsulfanyl-1-aminopropan, treatment with *t*-BuOK, provide the ring rearrangement to 6-member imide. Protection of the hydroxyl with TBS, followed by $NaIO_4$ gave the sulfoxide **24**. Further treatment of **24** with 2.2 equiv. of lithium hexamethyldisilazide (LHMDS) at -78 °C followed by quenching with water gave a mixture of stereoisomers **25** in the sulfur atom, being S_s isomer the major 65 %, against 15% R_s isomer, after column chromatography. The isomer S_s was reduced with $NaCNBH_3$ to give **2i)**.

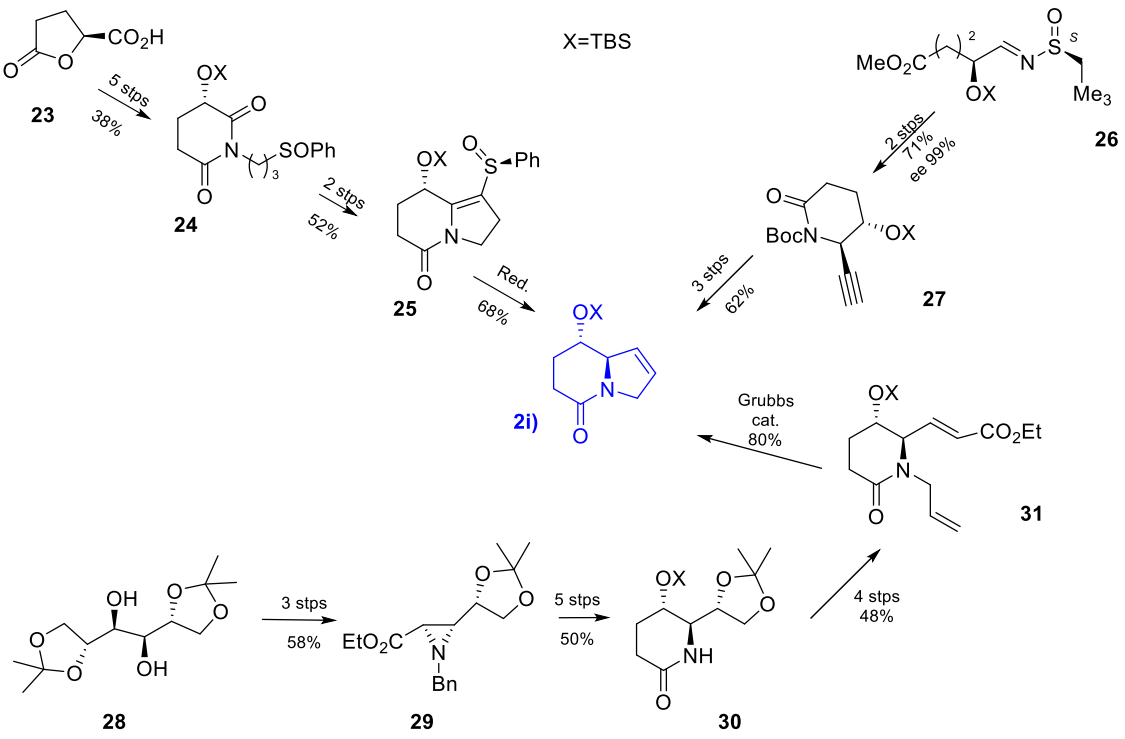

Scheme 6. The synthesis **2i)** precursor of swainsonine

The other one recent method to synthesis **2i)** precursor was proposed by S.P. Chavan *et al.* [24] in 2015. The chirality of precursor inherited from cheap and available D-mannitol diacetonide **28**. The starting material was subjected oxidative cleavage of diol with sodium periodate obtaining respective aldehyde. Followed the Wittig reaction with the formed aldehyde using bromophosphorane, affording the bromoester, which after a Gabriel-Cromwell reaction afforded the *trans*-aziridine **29**. In the next steps the ester group was reduced to aldehyde with DIBAL-H, the chain elongated by Wittig-Horn reaction, the aziridine ring was opened with TFA in acetonitrile-water 9:1 mixture, the alcohol function formed was protected with TBS, and the benzyl group was removed under catalytic hydrogenation to produce lactam **30**. Next two vicinal alkenic "arms" were introduced. First lactam **30** was *N*-alkylated with allyl bromide, then the diol obtained by isopropilidene acetal cleavage was oxidated to aldehyde with $NaIO_4$, then elongated by Wittig reaction to afford **31**. Under metathesis using Grubbs catalyst 2nd generation was obtained **2i)**.

In same year another group publish [25] a synthesis of swainsonine from α-chiral aldimines S_s **26**. Attack of an alkynyl Grignard reagent to the aldimine moiety followed by Boc_2O addition led to the formation of six-membered ring lactam **27**. The Grignard reaction's stereoselectivity is controlled by the α-alkoxyl relatively to the aldimine. Lactam **27** subjected to reduction with formation of an alkenic "arm". The Boc unit was removed and the allyl group was introduced in

nitrogen atom. The alkenic "arms" were submitted to metathesis under Grubbs catalyst 2nd generation to give **2i)**.

1.2.3 Synthesis of swainsonine from **1i)** and **2i)** precursors

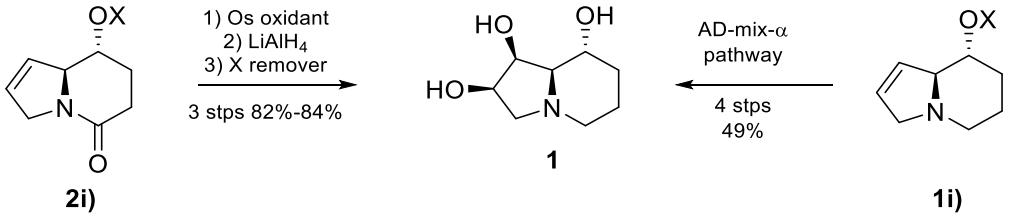

1i) X=TBSDPS, TIPS; **2i)** X=TBS

Scheme 7. Synthesis of swainsonine from **1i)** and **2i)** precursors

The main strategy for obtaining swainsonine (**Scheme 7**) from **1i)** are dihydroxylation by AD-mix-α (containing $K_2OsO_2(OH)_4$), followed by acetylation of the resulting mixture of diols to give a separable 9:1 diastereomeric mixture. In the final steps, acetate group are cleaved and the hydroxyl at C-8 is deprotected (X=TBSDPS). The yields for the 4 steps is 49% [21]. When X= TIPS the yield is slightly lower.

On the other hand, groups [23,25] which work **2i)** for synthesize swainsonine used a osmium catalyst in the presence of *N*-methylmorpholine *N*-oxide (NMMO) as the co-oxidant. The reaction is absolutely diastereoselective giving the product in very good yield. The amide was finally reduced, and the hydroxyl deprotected.

1.2.4 Synthesis swainsonine precursors: *N*-protected-3-oxy-2-piperidines **ii)**

Other one common precursor type **ii)** of the swainsonine are 3-substituted-piperidines, also these precursors, depending of R_1 (**Fig. 5**) group, can converted to **1i)** type precursors by Grubbs catalysis.

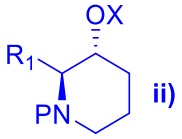

Fig. 5 *N*-protected-3-oxy-2-piperidines precursor

R. Martin and co-workers [26] in 2005 published a total synthesis of the swainsonine (**Scheme 8**) through **ii)** intermediate. The starting material is the epoxy alcohol **32** that was first subjected to carbamation with allyl isocyanate (**33**). In the presence of sodium *bis*(trimethylsilyl)amide the epoxide opens with formation of the oxazolidinone **34**. The alkenic "arms" go through ring-closing metathesis to form **35**. The Following steps involve hydrogenation the C=C bond, benzylation of the hydroxyl group, carbamate ring opening and protection of the piperidine nitrogen atom (**36**). The terminal hydroxyl group formed by removal of the carbamate was oxidized to aldehyde, submitted to Wittig reaction affording **ii)** in 92% of yield from **36**. The major *E* isomer was used for synthesis of swainsonine.

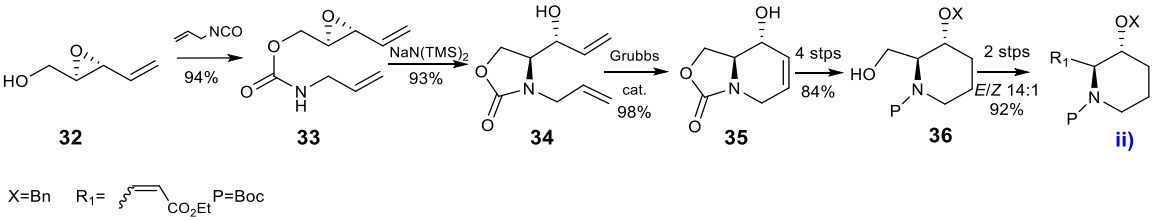

Scheme 8. R. Martin *et al.* synthesis

In the next year another synthesis of a precursor **ii)** was published [27] further converted into **1i)**. The starting chiral material **38** was obtained from (*E*)-vinyl sulfones (**37**) by treatment with AD-mix-β. To **38** was added allyl amine and β-styrenyl boronic acid in a borono-Mannich reaction furnishing **39**. In the next steps the hydroxyl was protected, TBDPS group was cleaved, and an Apple reaction was performed to give **ii)** by an intramolecular cyclization (**Scheme 9**).

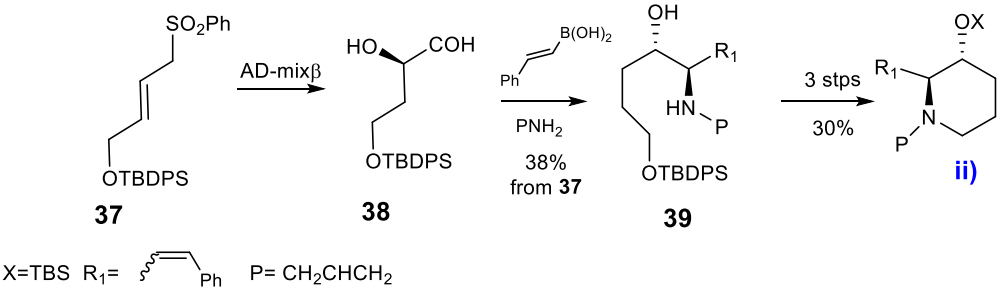

Scheme 9. C. W. G. Au *et al.* synthesis

The I. Dechamps *et al.* [28] in 2007 describe 2 pathways to the synthesis of the swainsonine from **ii)** (**Scheme 10**). The starting material is L-proline **40** which was converted into a common intermediate **41** in five steps: 1) esterification of carboxylic acid; 2) *N*-alkylation with trityl (Tr) chloride; 3) reduction of the ester function with $LiAlH_4$; 4) Swern oxidation of the formed alcohol to afford an aldehyde; 5) addition of vinyl-magnesium chloride to give the allylic alcohol **41**. The synthesis of **42** involves Tr substitution to benzoate (Bz), esterification of hydroxyl group with

acryloyl chloride followed by formation of a furanone *via* olefin metathesis with Grubbs catalyst. Stereo-selective oxidation of double bond with $NaIO_4$, under $RuCl_3$ catalysis, form a diol. This is protected with isopropilidene group, and the ring was opened with $LiAlH_4$ to form **43**. The primary alcohol was acetylated and the secondary hydroxyl was chlorinated with configuration retention using mesyl chloride in a microwave oven to form **44**. Under silver acetate in microwave at 120 °C an aziridinium salt occurs leading to ring expansion with formation of the piperidine compound **ii)**. A second protocol involves fewer steps and better yields. First in compound **41** the Tr group was substituted by the allyl group **45** (50% yield). Compound **45** led to an enantioselective ring expansion to form **ii)** under trifluoracetic anhydride and TEA, followed by NaOH.

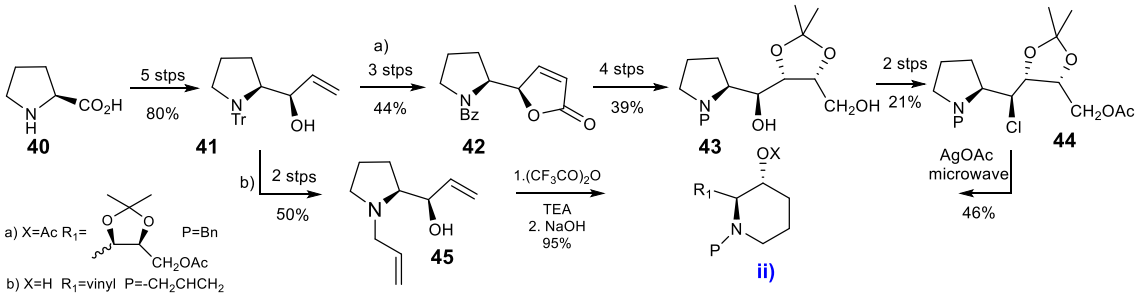

Scheme 10. I. Dechamps *et al.* synthesis

In 2009, Y. Tian *et al.* [29] published the full synthesis of swainsonine from *trans*-oxazoline **46**, obtained from D-serine. Compound **46** was submitted to hydrolysis for ring opening, the amine was protected to give **47**. In the next steps occurs: 1) a stereoselective hydroxylation with OsO_4 in presence NMMO; 2) benzoyl group migration to the primary alcohol position occurs in the reaction mixture by treatment with sat. aqueous Na_2SO_3 (**48**); 3) the formed diol was protected with a isopropylidene group; 4) TBS was cleaved, and the free hydroxyl group was oxidized with Dess-Martin periodinane (DMP) to give the aldehyde; 5) addition of allyl group to the aldehyde with allyltrimethylsilane forms **49**. The chiral alcohol function was protected with TBS, C=C double bound was oxidized under borane.SMe_2 complex to form the primary alcohol **50**. Treatment of **50** with mesyl chloride and trimethylamine (TEA) provide cyclization to **ii)** (**Scheme 11**).

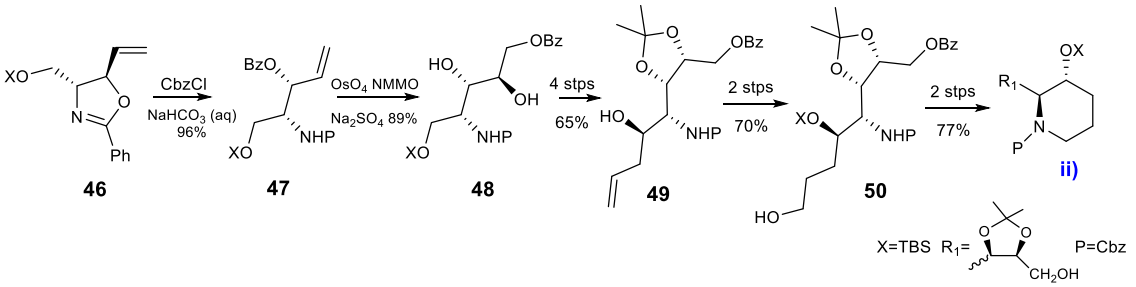

Scheme 11. Y. Tian *et al.* synthesis

The most recent literature for the synthesis of **ii)** intermediate [30] occurs from available enantiomerically pure aziridine **51** (**Scheme 12**). The ester group was converted into ketone *via* Weinreb synthesis giving **52**. The ketone group was reduced with $NaBH_4$, giving the respective alcohol in 99% *ee*. This group was protected with TBS. Under acetic acid in dichloromethane the aziridine was opened affording **53**. The terminal hydroxyl group was selectively deprotected by using mixture $AcOH/H_2O/THF$ (3:1:1). The primary alcohol was activated by mesylation. Under TEA an intramolecular cyclization occurs with formation piperidine. Further steps involve transformation the acetate group into vinyl, and *N*-deprotection followed by protection with Boc to give **ii)**.

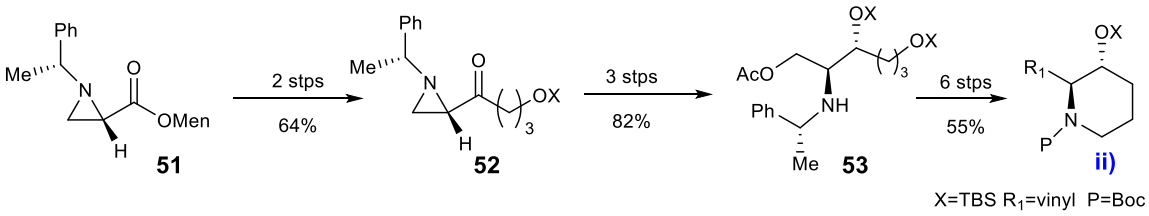

Scheme 12. H. G. Choi *et al.* synthesis

1.2.5 Synthesis swainsonine from 2-substituted piperidine **ii)** precursor

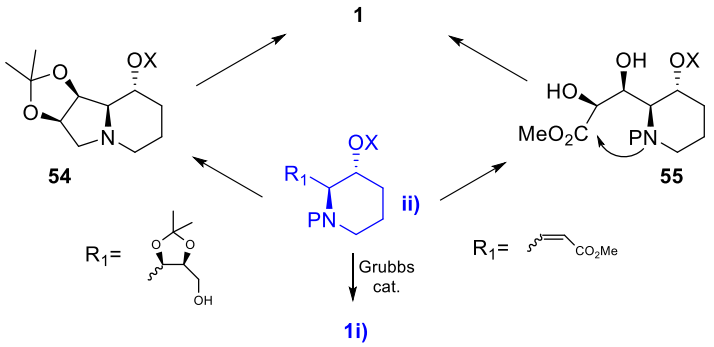

Scheme 13. Synthesis of swainsonine from 2-substituted piperidine **ii)**

Precursor of swainsonine **ii)** can be converted into **1i)** in case it bears two alkenic "arms" vinyl and allyl groups (as R_1/ P positions) *via* metathesis under Grubbs catalysis (**Scheme 13**). When compound **ii)** bears an α,β-unsaturated ester a *syn*-dihydroxylation of the alkenic moiety afford **55**. Cleavage of Boc with HCl in diethyl ether, followed by treatment with Hünig's base, diisopropiletilamina (DIEA), provide cyclization with formation of the bicyclic lactam. In the next steps the diol was protected, the carbonyl lactam reduced, and finally the hydroxyl groups were deprotected to give swainsonine (**1**). When precursor **ii)** bears a protected triol with terminal non-protected hydroxyl as R_1 and P as Cbz, simple procedure will apply. Treatment with mesyl chloride followed by hydrogenolysis with $Pd(OH)_2$ provide cyclization to give **54**. Hydroxyl deprotection afforded swainsonine in 69% yield over the three steps.

1.2.6 Synthesis of 2-substituted-pyrrolidine-3,4-diol precursor **iii)** of swainsonine

The 2-substituted-pyrrolidine-3,4-protected-diol **iii)** (**Fig. 6**) is one of mainframe to build up swainsonine. In many cases natural sugars are as the source of chirality.

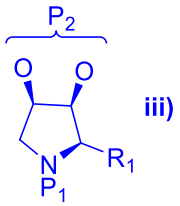

Fig. 6. 2-substituted-pyrrolidine-3,4-diol precursor

D-Glucose was used in the total synthesis of swainsonine starting from compound 2-epoxyfurane **56**, described by M. A. Alam and colleges [31] in 2008 (**scheme 14**). The epoxide group was treated with allyl magnesium chloride to provide epoxide opening with olefin chain propagation. The hydroxyl group formed was protected with the benzyl group, and isopropylidene was removed under HCl 10% in methanol providing the methyl acetal **57**. In the next steps, tetrahydrofuran ring was opened with 3 M HCl, the hemiacetal group was reduced, and the hydroxyl groups were mesylated to give **58**. The terminal alkene was dihydroxylated with OsO_4, the formed diol was subjected oxidative cleavage with sodium periodate, formed aldehyde was subjected subsequent reduction affording **59**. Simple treatment with benzylamine provide cyclization with formation of **iii)**.

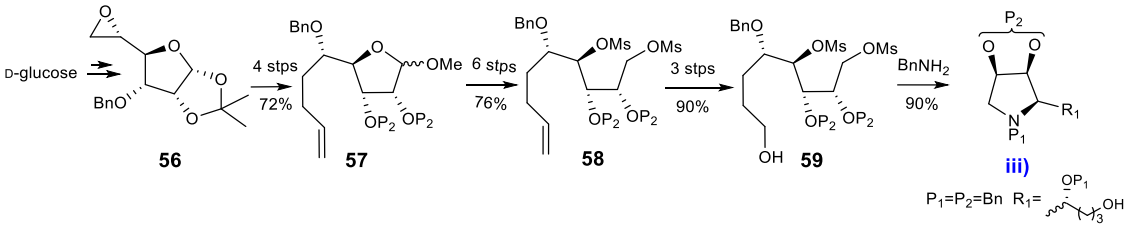

Scheme 14. M. A. Alam *et al.* synthesis

D. J. Wardrop & E. G. Bowen [32] in 2011 synthesized swainsonine from protected D-erythronolactone (**64**) (**Scheme 15**). Treatment of starting material with DIBAL-H afforded the respective D-erythrose. This, by Grignard reaction with vinylmagnesium bromide gave the free alcohol in 71% yield, dr=97:3. Protection of the terminal hydroxyl group with TBS gave **61**. Treatment of **61** with trimethyl orthoacetate in the presence of propionic acid as catalyst, undergo a Johnson–Claisen rearrangement to furnish **62**. The primary alcohol was oxidized to carboxylic acid *via* Dess-Martin and Pinnik sequence. Conversion of this material into the methyl hydroxamate **63** was obtained by reaction of isobutyl chloroformate followed by methoxylamine. Phenyliodine bis(trifluoroacetate) (PIFA) treatment provide a di-cyclization process with formation of **64**. Lithium borohydride reduction of **64** afforded swainsonine precursor **iii)**.

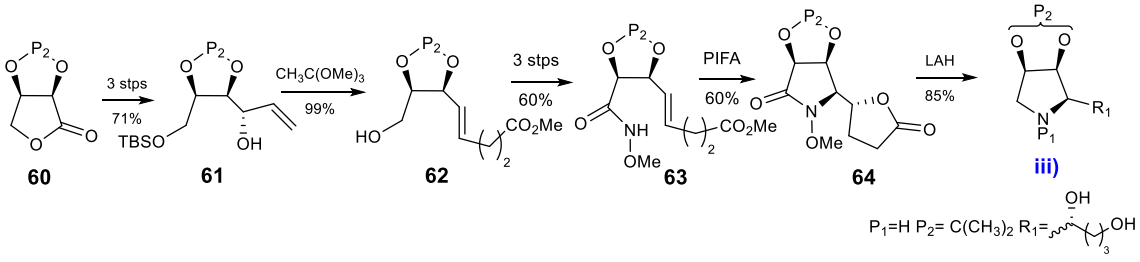

Scheme 15. D. J. Wardrop & E.G. Bowen synthesis

Another method for the synthesis of **iii)** starting from D-erythronolactone derivative **60** was published in same year [33] (**Scheme 16**). The authors did achieve the total synthesis of swainsonine in the following steps. Compound **60** was converted into the methyl hydroxamate with *N,O*-dimethylhydoxylamine and trimethylaluminium. The hydroxyl group was protected with TBS to give **65**. Treatment of **65** with (*R*$_s$)-*tert*-butanesulfinamide catalyzed by titanium(IV) ethoxide gave the chiral aldimine **66**. In the next steps **66** was coupled with **70**, generated *in situ* by lithiation of [3-(methoxymethoxy)prop-1-ynyl]-trimethylsilane (**69**) followed by transmetalation with $ZnBr_2$ affording **67** as a mixture of isomers. The major isomer was isolated in 75% yield. In the following steps, TMS attached to the alkyne moiety was cleaved, and the triple bond reduced to give **68**.

TBS was then removed, and the formed primary alcohol was mesylated. This compound under TEA cyclize to furnish **iii)**.

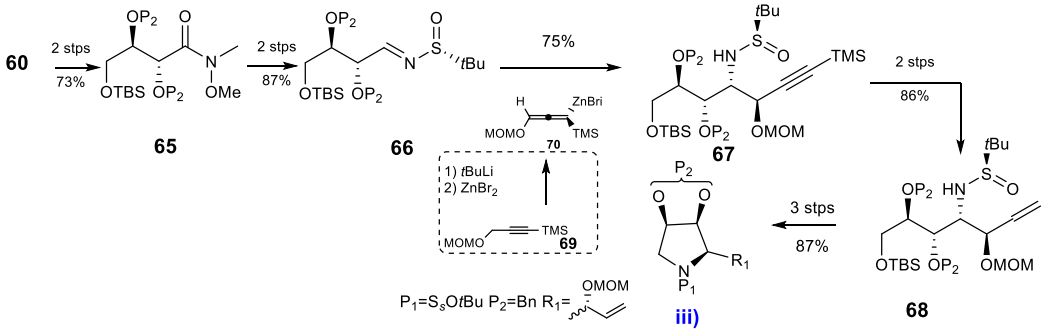

Scheme 16. J. Louvel *et al.* synthesis

M. Trajkovic and co-workers [34] described an elegant synthesis of swainsonine in 5 steps, 24% overall yield from achiral staring materials (**Scheme 17**). 1,3-Dioxanone **71** was coupled with protected aminoacetaldehyde **72** in presence of L-proline, as organocatalyst, providing formation of **73**, as a single diastereomer. Pyrrolidine **74** was formed by reductive amination, under H_2, Pd/C. Compound **74** was treated with *p*-TsOH in acetone to provide migration of the isopropylidene moiety with formation of **iii)**.

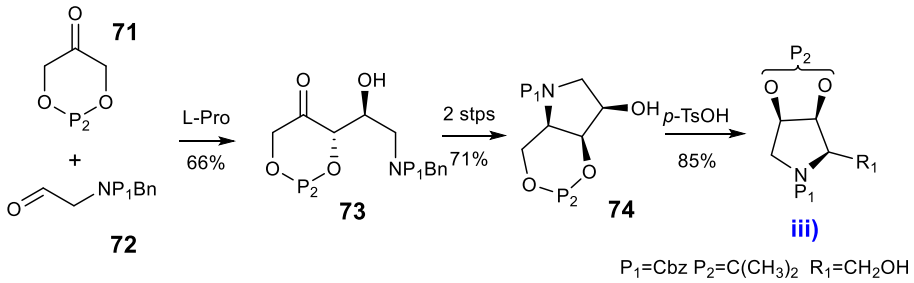

Scheme 17. M. Trajkovic *et al.* synthesis

Another synthesis for swainsonine from sugars pool was proposed by A. A. Ansari and Y. D. Vankar in same year [35] (**Scheme 18**). D-Galactal **75** was used as the staring material. The C=C bond under OsO_4/NMMO was dihydroxylated. Oxidative cleavage with sodium periodate, gave the aldehyde **76**. Reduction of compound **76** with sodium borohydride gave the respective diol, which was mesylated to afford **77**. Stereochemistry of the secondary mesylated alcohol was inverted by reaction with cesium acetate in the presence of 18-crown-6. The obtained compound was hydrolyzed and the free alcohol mesylated to give **78.** Addition of benzylamine promotes cyclization to **iii)**.

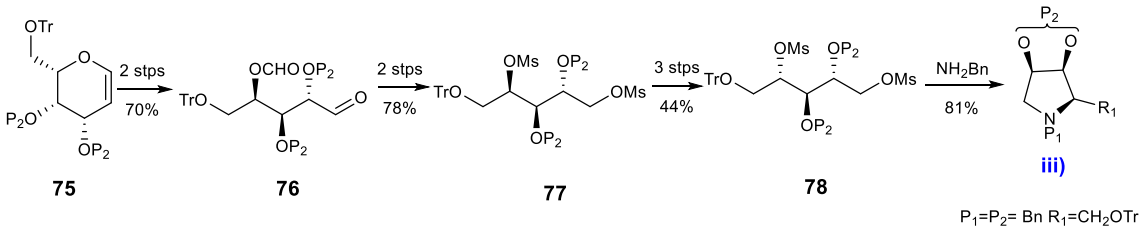

Scheme 18. A. A. Ansari and Y. D. Vankar synthesis

A recent report [36] of swainsonine synthesis is based on the cyclic nitrone **79** previously obtained from D-mannose in 6 steps and 43% overall yield (**Scheme 19**). Tautomerization of compound **79** into **80** occurred in two steps, 95% overall yield; reduction with $NaBH_4$ followed by oxidation with MnO_2. A second reduction with $NaBH_4$ furnished hydroxyamine **81** as a single product.

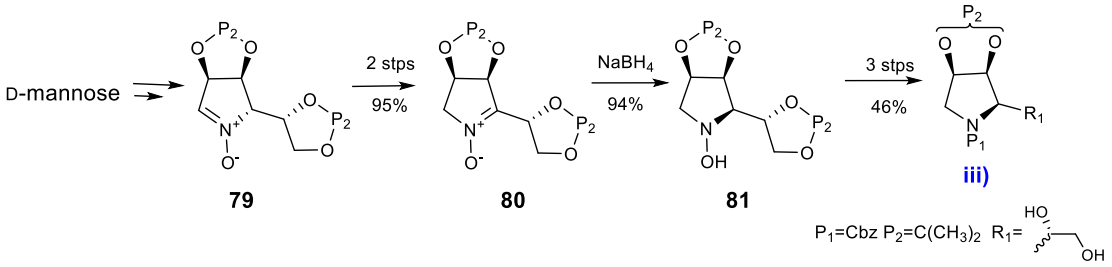

Scheme 19. B.C Qian *et al.* synthesis

The precursor of swainsonine **iii)** was obtained in three steps: reduction with zinc/$Cu(OAc)_2$, *N*-protection with Cbz group, followed by selective acetal cleavage with 1% H_2SO_4 in methanol.

1.2.7 Synthesis of swainsonine from **iii)** precursor

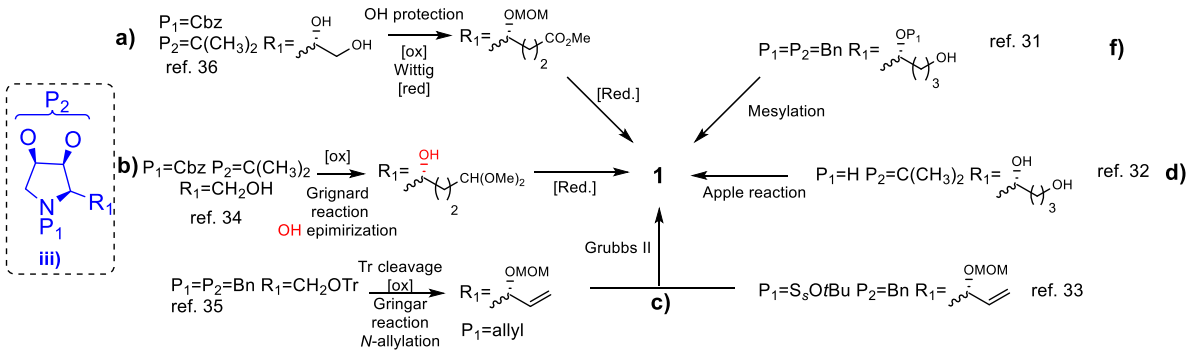

Scheme 20. Synthesis of swainsonine from **iii)** precursor

Scheme 20 resumes literature about swainsonine synthesis from **iii)** precursors in 5 pathways. The simplest pathway consists in direct cyclization into swainsonine core in case R_1 possess a free primary alcohol, either by mesylation or Apple reaction (**f**,**d**). In cases where R_1 and

P_1 can be transformed into alkenic groups, a metathesis will lead directly to the swaisonine core (cases **c**). In one case, **b**), when R_1 is a 4-carbon atom chain possessing a dimethyl acetal group at the terminal position, and a hydroxyl group at C-1', with P_1= Cbz group and P_2 = isopropylidene, hydrogenolysis in ethanol /HCl led to swainsonine. Finally, in case **a**), when R_1 is a 4-carbon atom chain with terminal ester group, and a hydroxyl protected MOM group at C-1', P_1 = Cbz, and P_2 = isopropylidene a two reduction processes and two acid treatments afforded swainsonine in fairly good yields. In some cases swainsonine (**1**) was obtained after further group's deprotection.

1.2.8 Other synthesis of swainsonine

There are two cases of the swainsonine synthesis not included in previous categories. P. K. Sharma and co-workers [37] started from **82**, a derivative of D-glyceraldehyde. The reactions were carried out on a kg scale. First, the primary alcohol was transformed into azide **83** by a Mitsunobu reaction in 85% of yield. The azide was refluxed in toluene for 20 h providing cyclization. After ester moiety hydrolysis with NaOH the carboxylic acid **84** was formed. By acetic acid treatment at 110 °C a second cyclization took place to give the bicyclic lactam **85** in 80% yield from **84**. Subsequent treatment of **85** with an excess of borane/THF complex at < 5 °C followed by aqueous NaOH and 30% aqueous H_2O_2 result in the formation of **86** in 66% yield. In the final step the vicinal diol was deprotected with HCl to afford swainsonine (98 %) (**Scheme 21**).

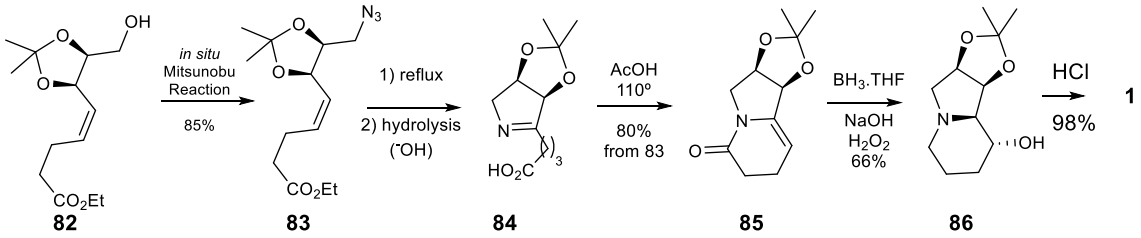

Scheme 21. P. K. Sharma *et al.* synthesis

H. Guo and G. A. O'Doherty [38] synthesized swainsonine starting with achiral materials: 2-lithiumfuran and γ-butyrolactone. Condensation of the compounds afforded 2-substituted furan **87** (**scheme 22**). The alcohol included in the structure was protected with TBSCl, then the ketone was stereoselectively reduced by **Noyori (*S,S*)** catalyst giving **88**. Under Achmatowicz conditions: *N*-Bromosuccinimide (NBS) in THF/H_2O the furan ring rearrange to pyranone **89** in 84% yield. A diastereoselective protection of the anomeric position was performed in two-steps: acylation with $(Boc)_2O$ followed by reduction with Pd/PPh_3. The azide was incorporated at C-4 of compound **90**

after reduction of the ketone unit with $NaBH_4$, followed by reaction with methyl chloroformate to give a carbonate. Then, using stereoselective Sinou's methodology with palladium catalysis $(Pd(allyl)Cl)_2$/1,4-bis(diphenylphosphino)butane was obtained **91** in 52% overall yield for the three steps. Subsequently the hydroxyl was deprotected and mesylated to afford **92**; the double bond was dihydroxylated to give **93**; finally **93** was subjected to high pressure hydrogenolysis to give swainsonine.

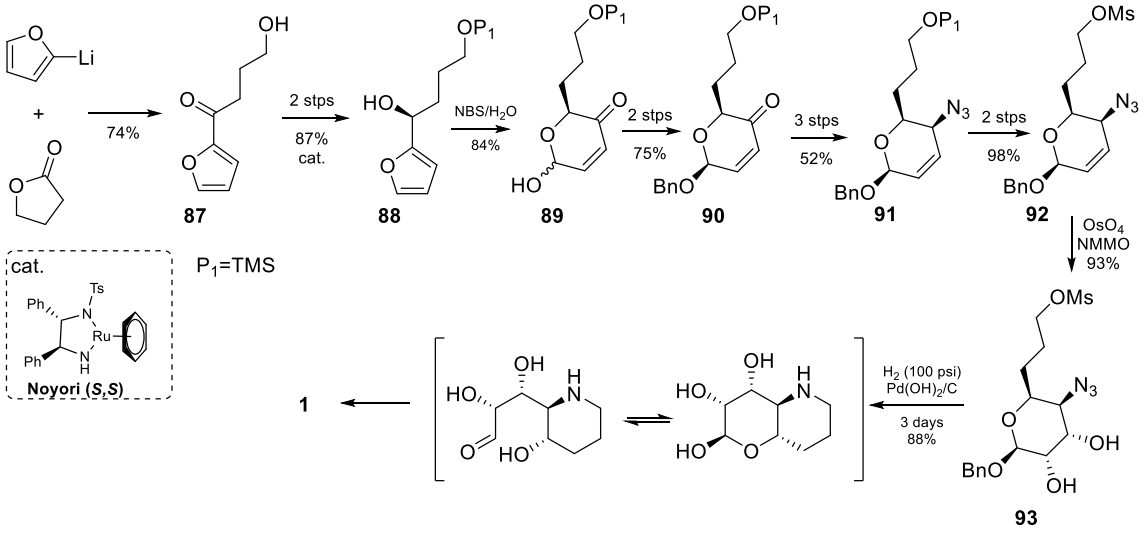

Scheme 22. H. Guo & G. A. O'Doherty synthesis

1.3 Synthesis of substituted swainsonine

After understanding the potential of the swainsonine molecule, several modifications of its structure were conducted in order to improve activity, biological selectivity together with evaluation of the enzymatic mechanisms. As in the previous section, this part will be considered solely works after Pyne's review referred to (+)- and (-)-swainsonines.

1.3.1 Synthesis of 5-substituted analogues

Fujita *et al.* [39] reported the synthesis of 5-substituted swainsonines as well their biological evaluation. The chemical sequence starts from **95**, obtained from commercially available D-erythrolactone derivative **94**. In the first step occurs a non-stereoselective reduction of lactone with

DIBAL-H and further etherification of the anomeric position with acetone dimethyl acetal to afford **96** in quantitative yield. Hydrogenolysis of the azido group under palladium hydroxide provides cyclization to give compound **97**, the key intermediate for synthesis 5-substituted swainsonine. (**Scheme 23**)

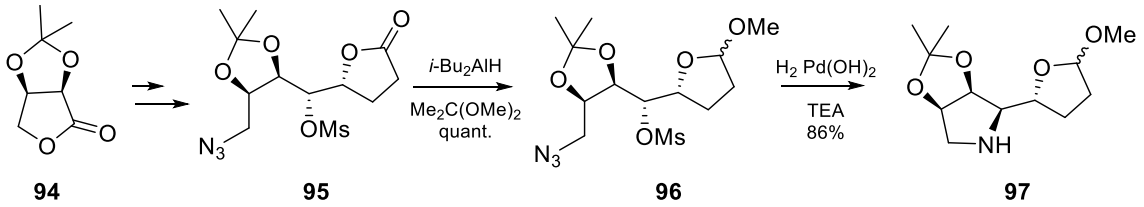

Scheme 23. The synthesis of key precursor for 5-substituted swainsonine

Under acid treatment in protic solvent **97** suffered a cyclization with formation of an imonium salt, in equilibrium with the respective enamine. Mannich addition of ketones occurred to afford products **98** in moderate to low yields. Epimerization at C-5 occurs in reasonable yield by incubation of **98** in MeOH for several days or by treatment with basic ion-exchange resin (Dowex 1X8) for several hours, to give the isomer **99** (**Scheme 24**).

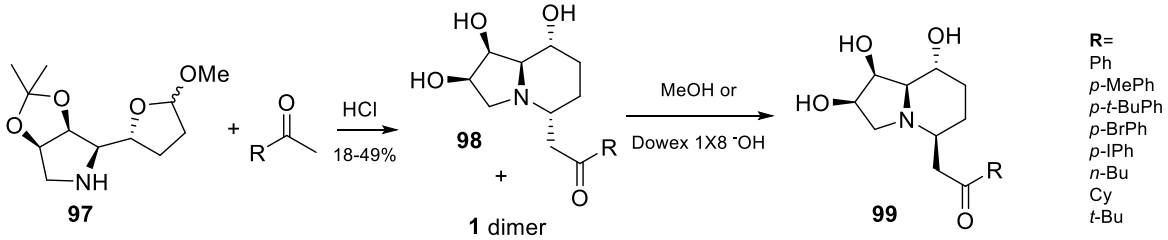

Scheme 24. Fujita *et al.* synthesis of 5-substituted swainsonine by Mannich reaction

Evaluation of compounds **98** in α-mannosidase from Jack beans, with R= *p*-MePh, *p*-*t*-BuPh, *p*-BrPh, *p*-IPh showed good inhibition activity IC_{50}=0.22-0.42 μM (swainsonine IC_{50}=0.25 μM), but its isomer **99** is less active (IC_{50}=0.91-3.29 μM).

1.3.2 Synthesis of L-swainsonine 6-substituted- and 6,6,7-trisubstituted L-swainsonine analogues

A. E. Hakansson *et al.* [40] synthesized 6- and 6,6,7-trisubstituted analogues of the L-swainsonine from readily available glucoheptolactone **100**. Pyrrolidine **101**, the key intermediate, is obtained in a sequence of hydroxyl protection/deprotection, and incorporation of the nitrogen atom at the last step with benzylamine. Pyrrolidine **101** was converted into **102** in two steps: 1)

oxidative cleavage with sodium periodate; 2) Wittig olefination with $Bu_3P=C(Me)CO_2Me$ afford the conjugated esters in 1 (*Z*) : 4 (*E*) ratio, and 81% combined yield. The mixture was submitted to hydrogenolysis under palladium hydroxide to afford separable *R*/ *S* bicyclic lactams **103**, in 43% (*R*)/ 28% (*S*) yields. Each lactam was reduced under borane–tetrahydrofuran complex, and deprotected with TFA to afford (+)-L-6-methylswainsonines **104** in 77% (*R*), and 81% (*S*) yield (**Scheme 25**). L-Swainsonine could also be obtained following the same sequence from **101** using $Bu_3P=CHCO_2Me$ in the Wittig reaction. Enzymatic inhibition studies of *R* and *S* **104** isomers showed a very good activity for the *R* compound towards α-L-rhamnosidase IC_{50}=34 nM, K*i*=32 nM, but the *S* isomer inhibition activity decreased in two folds of magnitude to IC_{50}=1.17 μM K*i*=1.10 μM. The inhibition of α-L-rhamnosidase by L-swainsonine is less active then the *R* isomer ahead, IC_{50}=130 nM K*i*=450 nM.

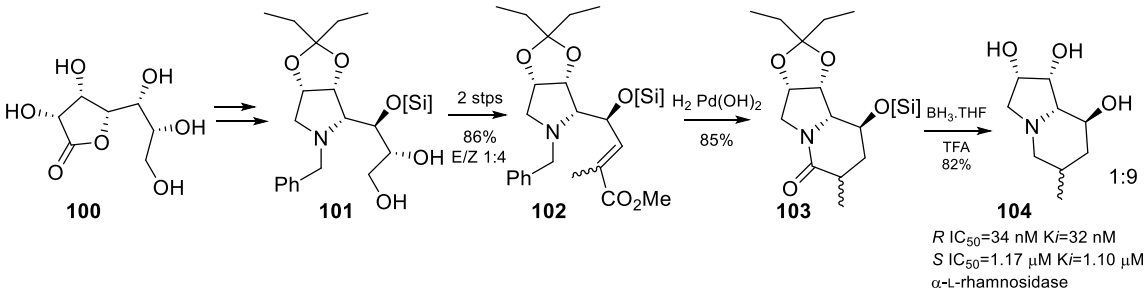

Scheme 25. A. E. Hakansson *et al.* L-6-methylswainsonine synthesis

Intermediate ***E*-102** was used for the synthesis of L-6,6,7-trisubstituted swainsonines (**Scheme 26**). Under osmilation conditions were obtained a separable mixture of lactones **106** and **109** in 3:1 ratio. Hydrogenation of each lactone under $Pd(OH)_2$ followed by treatment with potassium carbonate in methanol led to lactams **107** and **110**. Final products were obtained by reduction with borane–tetrahydrofuran complex. Isomer **108** was obtained in 22% of yield and isomer **111** was also isolated, but no yield reported. Inhibition activity of **108** and **111** against α-L-rhamnosidase is IC_{50}=21.3 μM for **108**, and IC_{50}=9.2 μM for **111**, both lower than for 6-methylswainsonines.

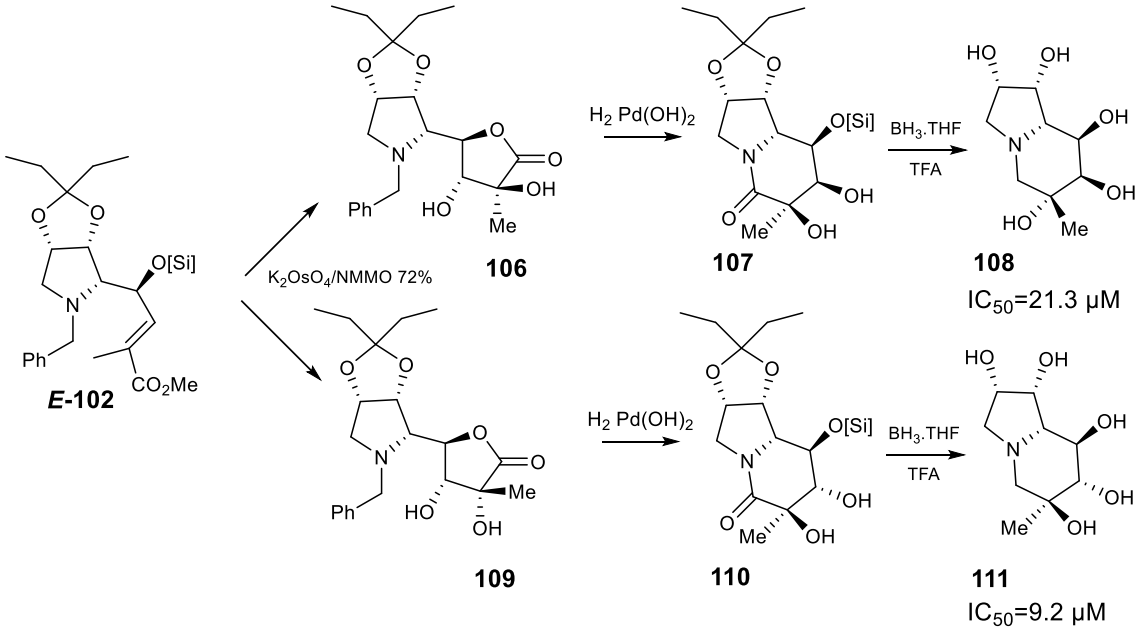

Scheme 26. Synthesis of (+)-L-6,6,7-trisubstituted swainsonine analogues

1.3.3 Synthesis of 7-disubstituted D-swainsonine analogues

Alessandro Tinarelli and Claudio Paolucci [41] synthesized 7-acetamidoswainsonine analogue (**Scheme 27**) from lactam **112** described in literature [42]. Reflux of lactam **112** under DMP and diazabicycloundecene (DBU) afforded **113** in 88% yield. The α,β-unsaturated carbonyl unit was subjected to Michael addition to give **114** (84%) and **115** (78%). Additions are highly stereoselective processes. The synthesis of a swainsonine analogue was concluded only with **114**. The azide group and carbonyl were subjected to a tandem reduction with borane-dimethyl sulfide. The isopropylidene group was removed under HCl treatment. Subsequent treatment of the deprotected compound with acetic anhydride led to amine and hydroxide acetylations. The final product **116** was obtained after alkaline treatment in 56% overall yield for the three last steps.

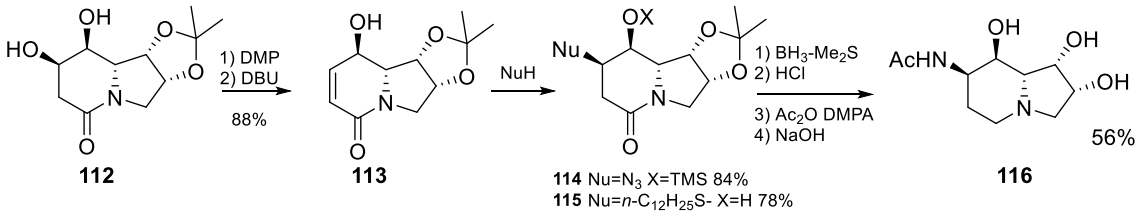

Scheme 27. Synthesis of 7-substituted D-swainsonine analogues

1.4 References

(1) Guengerich, F. P.; DiMari, S. J.; Broquist, H. P. Isolation and Characterization of a 1-Pyrindine Fungal Alkaloid. *J. Am. Chem. Soc.* **1973**, *95* (6), 2055–2056.

(2) Schneider, M. J.; Ungemach, F. S.; Broquist, H. P.; Harris, T. M. (1S,2R,8R,8aR)-1,2,8-Trihydroxyoctahydroindolizine (Swainsonine), an α-Mannosidase Inhibitor from Rhizoctonia Leguminicola. *Tetrahedron* **1983**, *39* (I), 29–32.

(3) Colegate, S. M.; Dorling, P. R.; Huxtable, C. R. A Spectroscopic Investigation of Swainsonine: An a-Mannosidase Inhibitor Isolated from Swainsona Canescens. *Aust. J. Chem.* **1979**, No. 32, 2257–2264.

(4) Dorling, P. R.; Colegate, S. M.; Huxtable, C. R. The Biological Activity of Swainsonine: An Indolizidine Alkaloid Isolated from Swainsona Canescens. *Toxicon,* **1983**, 93–96.

(5) Dorling, P. R.; Huxtable, C. R.; Colegate, S. M. Inhibition of Lysosomal A-Mannosidase by Swainsonine , an Indolizidine Alkaloid Isolated from Swainsona Canescens. **1980**, *191*, 649–651.

(6) Panter, K. E.; Welch, K. D.; Gardner, D. R. Poisonous Plants: Biomarkers for Diagnosis. In *Biomarkers in Toxicology*; 2014; pp 563–589. https://doi.org/10.1016/B978-0-12-404630-6.00033-6.

(7) Nargs.org. North American Rock Garden Society https://nargs.org/plant/oxytropis-sericea (accessed Aug 20, 2019).

(8) Le.Loup.Gris. Wikimedia.org https://commons.wikimedia.org/wiki/File:Astragalus_dasyanthus_habitus_1.jpg (accessed Aug 20, 2019).

(9) Molyneux, R. J.; James, L. F. Loco Intoxication: Indolizidine Alkaloids of Spotted Locoweed (Astragalus Lentiginosus). *Science,* **1982**, *216* (4542), 190–191.

(10) Creamer, R.; Baucom, D.; Welsh, S. L.; Cook, D. Relationship Between the Endophyte Embellisia Spp . and the Toxic Alkaloid Relationship Between the Endophyte Embellisia Spp . and the Toxic Alkaloid Swainsonine in Major Locoweed Species (Astragalus and Oxytropis). *J. Chem. Ecol,* **2008**, No. 34, 32–38. https://doi.org/10.1007/s10886-007-9399-6.

(11) Rooprai, H. K.; Kandanearatchi, A.; Maidment, S. L.; Christidou, M. Evaluation of the Effects of Swainsonine , Captopril , Tangeretin and Nobiletin on the Biological Behaviour of Brain Tumour Cells in Vitro. **2001**, 29–39.

(12) Elsen, J. M. H. Van Den; Kuntz, D. A.; Rose, D. R. Structure of Golgi a -Mannosidase II : A Target for Inhibition of Growth and Metastasis of Cancer Cells. *Euro. Mol. Biol. Org.* **2001**, *20* (12), 3008–3.

(13) Sun, J.; Zhu, M.; Wang, S.; Miao, S.; Xie, Y.; Wang, J. Inhibition of the Growth of Human Gastric Carcinoma in Vivo and in Vitro by Swainsonine. *Phytomedicine* **2007**, *14*, 353–359. https://doi.org/10.1016/j.phymed.2006.08.003.

(14) Shaheen, P. E.; Stadler, W.; Elson, P.; Knox, J.; Winquist, E.; Ronald, M. Phase II Study of the Efficacy and Safety of Oral GD0039 in Patients with Locally Advanced or Metastatic Renal Cell Carcinoma. *Invest. New Drugs* **2005**, *23*, 577–581.

(15) Kino, T.; Inamura, N.; Nakahara, K.; Kiyoto, S.; Goto, T.; Terano, H.; Kohsaka, M.; Aoki, H.; Imanaka, H. Studies of an Immunomodulator, Swainsonine. II. Effect of Swainsonine on Mouse Immunodeficient System and Experimental Murine Tumor. *J. Antibiot.* **1985**, No. 38, 936–940.

(16) Pyne, S. Recent Developments on the Synthesis of (-)-Swainsonine and Analogues. *Curr. Org. Synth.* **2005**, *2* (1), 39–57. https://doi.org/10.2174/1570179052996900.

(17) Wu, C.; Feng, K.; Lu, D.; Yan, D.; Han, T.; Zhao, B. Reproductive Toxicities Caused by Swainsonine from Locoweed in Mice. *Biomed Res. Int.* **2016**, *2016*, 6824374. https://doi.org/10.1155/2016/6824374.

(18) Ceccon, J.; Greene, A. E.; Poisson, J. F. Asymmetric [2 + 2] Cycloaddition: Total Synthesis of (-)-Swainsonine and (+)-6-Epicastanospermine. *Org. Lett.* **2006**, *8* (21), 4739–4742. https://doi.org/10.1021/ol0617751.

(19) Kwon, H. Y.; Park, M.; Lee, B.; Youn, J. Asymmetric Iodocyclization Catalyzed by Salen – Cr III Cl : Its Synthetic Application to Swainsonine. *Chem. Eur. J.* **2008**, *14*, 1023–1028. https://doi.org/10.1002/chem.200701199.

(20) Bates, R. W.; Dewey, M. R. A Formal Synthesis of Swainsonine by Gold-Catalyzed Allene Cyclization. *Org. Lett.* **2009**, *11* (16), 3706–3708. https://doi.org/10.1021/ol901094h.

(21) Archibald, G.; Lin, C. P.; Boyd, P.; Barker, D.; Caprio, V. A Divergent Approach to 3-Piperidinols: A Concise Syntheses of (+)-Swainsonine and Access to the 1-Substituted Quinolizidine Skeleton. *J. Org. Chem.* **2012**, *77* (18), 7968–7980. https://doi.org/10.1021/jo3011914.

(22) Dhand, V.; Draper, J. A.; Moore, J.; Britton, R. A Short, Organocatalytic Formal Synthesis of (-)-Swainsonine and Related Alkaloids. *Org. Lett.* **2013**, *15* (8), 1914–1917. https://doi.org/10.1021/ol400566j.

(23) Chooprayoon, S.; Kuhakarn, C.; Tuchinda, P.; Reutrakul, V.; Pohmakotr, M. Asymmetric Total Synthesis of (+)-Swainsonine. *Org. Biomol. Chem.* **2011**, *9* (2), 531–537. https://doi.org/10.1039/c0ob00388c.

(24) Chavan, S. P.; Khairnar, L. B.; Pawar, K. P.; Chavan, P. N.; Kawale, S. A. Enantioselective Syntheses of (R)-Pipecolic Acid, (2R,3R)-3-Hydroxypipecolic Acid, β-(+)-Conhydrine and (-)-Swainsonine Using an Aziridine Derived Common Chiral Synthon. *RSC Adv.* **2015**, *5* (62), 50580–50590. https://doi.org/10.1039/c5ra06429e.

(25) Si, C. M.; Mao, Z. Y.; Dong, H. Q.; Du, Z. T.; Wei, B. G.; Lin, G. Q. Divergent Method to Trans -5-Hydroxy-6-Alkynyl/Alkenyl-2-Piperidinones: Syntheses of (-)-Epiquinamide and (+)-Swainsonine. *J. Org. Chem.* **2015**, *80* (11), 5824–5833. https://doi.org/10.1021/acs.joc.5b00803.

(26) Martín, R.; Murruzzu, C.; Pericàs, M. A.; Riera, A. General Approach to Glycosidase Inhibitors. Enantioselective Synthesis of Deoxymannojirimycin and Swainsonine. *J. Org. Chem.* **2005**, *70* (6), 2325–2328. https://doi.org/10.1021/jo048172s.

(27) Au, C. W. G.; Pyne, S. G. Asymmetric Synthesis of Anti-1,2-Amino Alcohols via the Borono-Mannich Reaction: A Formal Synthesis of (-)-Swainsonine. *J. Org. Chem.* **2006**, *71* (18), 7097–7099. https://doi.org/10.1021/jo0610661.

(28) Dechamps, I.; Pardo, D. G.; Cossy, J. Enantioselective Ring Expansion of Prolinol Derivatives . Two Formal Syntheses of (-)-Swainsonine. *Tetrahedron* **2007**, *63*, 9082–9091. https://doi.org/10.1016/j.tet.2007.06.086.

(29) Tian, Y.; Joo, J.; Kong, B.; Pham, V.; Lee, K.; Ham, W. Asymmetric Synthesis of (-)-Swainsonine. *J. Org. Chem.* **2009**, *74*, 3962–3965. https://doi.org/10.1021/jo802800d.

(30) Choi, H, G.; Kwon, J, H.; Kim, J, C.; Lee, K, W.; Eum, H.; Ha, H. A Formal Synthesis of (-) -Swainsonine from a Chiral Aziridine. *Tetrahedron Lett.* **2010**, *51* (25), 3284–3285. https://doi.org/10.1016/j.tetlet.2010.04.069.

(31) Alam, M. A.; Kumar, A.; Vankar, Y. D. Total Synthesis of L-(+)-Swainsonine and Other Indolizidine Azasugars from D -Glucose. *Eur. J. Org. Chem.* **2008**, No. 29, 4972–4980. https://doi.org/10.1002/ejoc.200800649.

(32) Wardrop, D. J.; Bowen, E. G. Nitrenium Ion-Mediated Alkene Bis-Cyclofunctionalization: Total Synthesis of (-)-Swainsonine. *Org. Lett.* **2011**, *13* (9), 2376–2379. https://doi.org/10.1021/ol2006117.

(33) Louvel, J.; Chemla, F.; Demont, E.; Ferreira, F.; Pérez-Luna, A. Synthesis of (-)-Swainsonine and (-)-8épi-Swainsonine by the Addition of Allenylmetals to Chiral α,β-Alkoxy Sulfinylimines. *Org. Lett.* **2011**, *13* (24), 6452–6455. https://doi.org/10.1021/ol202747p.

(34) Trajkovic, M.; Balanac, V.; Ferjancic, Z.; Saicic, R. N. Total Synthesis of (+)-Swainsonine and (+)-8-Epi-Swainsonine. *RSC Adv.* **2014**, *4* (96), 53722–53724. https://doi.org/10.1039/c4ra11978a.

(35) Ansari, A. A.; Vankar, Y. D. Synthesis of Pyrrolidine Iminosugars, (-)-Lentiginosine, (-)-Swainsonine and Their 8a-Epimers from d-Glycals. *RSC Adv.* **2014**, *4* (24), 12555–12567. https://doi.org/10.1039/c3ra47555g.

(36) Qian, B. C.; Kamori, A.; Kinami, K.; Kato, A.; Li, Y. X.; Fleet, G. W. J.; Yu, C. Y. Epimerization of C5 of an: N -Hydroxypyrrolidine in the Synthesis of Swainsonine Related Iminosugars. *Org. Biomol. Chem.* **2016**, *14* (19), 4488–4498. https://doi.org/10.1039/c6ob00531d.

(37) Sharma, P. K.; Shah, R. N.; Carver, J. P. Scale-up Synthesis of Swainsonine: A Potent #-Mannosidase II Inhibitor. *Org. Process Res. Dev.* **2008**, *12* (5), 831–836. https://doi.org/10.1021/op800059y.

(38) Guo, H.; O'Doherty, G. A. De Novo Asymmetric Synthesis of D- and L-Swainsonine. *Org. Lett.* **2006**, *8* (8), 1609–1612. https://doi.org/10.1021/ol0602811.

(39) Fujita, T.; Nagasawa, H.; Uto, Y.; Hashimoto, T.; Asakawa, Y.; Hori, H. Synthesis of the New Mannosidase Inhibitors, Diversity-Oriented 5-Substituted Swainsonine Analogues, via Stereoselective Mannich Reaction. *Org. Lett.* **2004**, *6* (5), 827–830. https://doi.org/10.1021/ol049947m.

(40) Hakansson, A. E.; Ameijde, J. Van; Horne, G.; Nash, R. J.; Ha, A. E.; Wormald, M. R.; Kato, A.; Besra, G. S.; Fleet, G. W. J. Synthesis of the Naringinase Inhibitors L-Swainsonine and Related 6-C-Methyl-L-Swainsonine Analogues : (6R)- C-Methyl-L-Swainsonine Is a More Potent Inhibitor of L-Rhamnosidase by an Order of Magnitude than L-Swainsonine. *Tetrahedron Lett.* **2008**, *49*, 179–184. https://doi.org/10.1016/j.tetlet.2007.10.142.

(41) Tinarelli, A.; Paolucci, C. Stereoselective Michael Addition of Carbon-, Nitrogen-, Oxygen-, and Sulfur-Centered Nucleophiles on Enantiopure Hydroxylated 6,7-Dehydro-5- Oxoindolizidine. Synthesis of Carbon- or Hetero-7-Substituted Swainsonine Analogues. *J. Org. Chem.* **2006**, *71* (17), 6630–6633. https://doi.org/10.1021/jo060511p.

(42) Paolucci, C.; Mattioli, L. Stereoisomeric Sugar-Derived Indolizines as Versatile Building Blocks: Synthesis of Enantiopure Di- and Tetrahydroxyindolizidines. *J. Org. Chem.* **2001**, *66* (14), 4787–4794. https://doi.org/10.1021/jo0016428.

Chapter II: Results and discussion. Theoretical studies.

"When the theory coincides with the experiment, this is no longer a discovery, but a closure of the topic."
Pyotr Kapitsa

2.1 Introduction

Glycoprocessing enzymes are an interesting therapeutic target because they are responsible for the metabolism of complex carbohydrate structures involved in many biochemical recognition processes.

Natural alkaloid swainsonine (swa) is known as a potent and selective inhibitor of glycoside hydrolases from the GH family 38 [1,2]. The effect of swainsonine on oligosaccharide processing was also elucidated [3]. Also, its role as anti-tumor agent was disclosed in Chapter 1.

However, swa and all other known GH38 α-mannosidase inhibitors exhibit also a serious side effect. *i.e.* they inhibit broad-specificity GH 38 lysosomal α-mannosidase (LMan) (EC 3.2.1.24) [4,5]. This fact limits their use as therapeutics due to an accumulation of mannose-containing oligosaccharides in tissues and serum, and their appearance in urine, provoking lysosomal storage diseases.

The known characteristics and effect of swa are a start point in the design of swa based compounds with improved profile, *i.e.*, presenting decreased toxicity and high selectivity towards Golgi α-mannosidase. In this sense, the major aim in using computational techniques is understanding broadly both enzymes and the interaction pattern with swa and designed analogs. Molecular modelling (MM) methods can disclose in detail aspects of Golgi and lysosomal mannosidases, as their dynamic behavior, active site characteristics and the interactions with inhibitors. Many MM techniques were used in this work to study the properties of interest.

One major challenge in the study of this type of inhibitor, in its ultimate target, the human Golgi and lysosomal mannosidases, refer to the difficult to purify mammalian samples in a quantity suitable for physical studies [6]. Because of this fact, most of studies are performed in glycosidases from other organisms, typically from drosophila (*Drosophila melanogaster*) or Jack bean (*Canavalia ensiformis*).

Due to the know structural conservation among organisms, it is possible to predict the structure of human Golgi and lysosomal mannosidases using threading search algorithms, implemented in Protein Structure Prediction (PSP) programs.

Globally, Golgi α-mannosidase is a type II transmembrane protein, with approximately 125 kDa in size and located in the Golgi apparatus. GMII consists of a N-terminal α/β domain, a three α-helix bundle and an all-β C-terminal domain forming a single compact entity, connected by five internal disulfide bonds [6]. Structurally, lysosomal is very similar and located in lysosomes, although small in amino acid sequence. Concerning the active site, both enzymes has a Zn^{2+} ion essential

to the biological activity and hydrolase reaction, as the substrates complexed with this ion, and then the reaction occurs.

To understand what could be behind of an optimum binding and selectivity, we study the enzymes by using different techniques, such as, PSP/homology modelling, virtual screening of inhibitors *via* molecular docking, molecular dynamics (MD) simulation of the most promising inhibitor-target complexes and analysis tools. **Scheme 1** helps to follow our rational and protocol for computational studies.

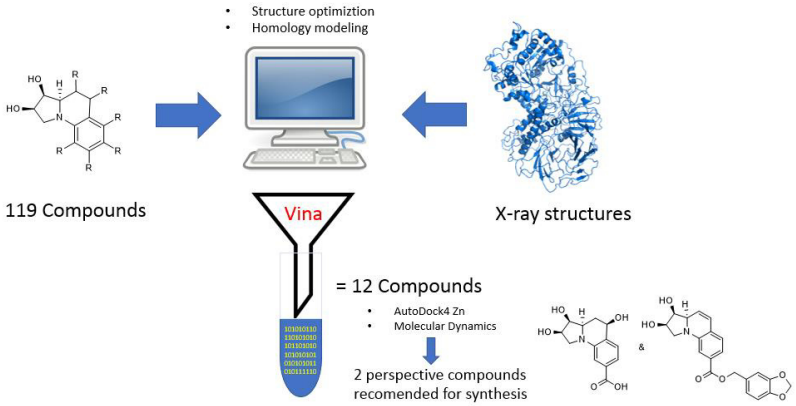

Scheme 1. Representative workflow of the protocol/computational experiments used in this study

2.2 Results and discussion

To accomplish the protocol described in **Scheme 1**, several tasks were performed. First, were designed hexahydropyrroloquinoline (HHPQ) type compounds that could be synthesized by the method described in next chapter, creating a library with 119 possible inhibitors. After this, molecular docking using two different methods were carried out to dock these compounds against the mannosidases. This was done using experimental determined structures and the human models proposed here.

Concerning the human models, we proposed structures for Golgi α-mannosidase II (hGMII) and Lysosomal mannosidase (hLM) *via* homology modelling, as this is the ultimate target for applications of the designed inhibitors. These models were equilibrated through molecular dynamics simulations.

Finally, were selected the best candidates and simulated the inhibitor-enzyme complexes, to achieve a global understand about these systems.

2.2.1 Protein structure prediction of human enzymes

Currently exist two X-ray structures of the enzymes addressed in this study with good resolution: Golgi α-mannosidase II (GMII) of drosophila PDB ID:3blb and bovine lysosomal α-mannosidase (LM) (1o7d). However, none experimental solved structure is available for the equivalent human glycosidases.

To study the possible behavior of some partial analogues of the swa with the human enzymes, PSP techniques were performed. This was done using I-Tasser server [7–9], a program that generates model structures by homology modeling and call upon templates from the Protein Data Bank [10]. To use this method, it is necessary submit into the server the full human sequence of our target protein that were achieved through UniProt Database [11]. For Golgi, the entry Q16706 was used, and for lysosomal, the code O00754.

After that, the program search for threading templates to predict the models. In the case of human Golgi α-mannosidase the templates were the proteins with the following codes: 3dx4, 5jm0, 2ow6 and 3bvx. For human lysosomal α-mannosidade, I-Tasser used: 6b9o, 3dx4 and 3bvx. Three of these templates are high resolution X-ray structures of Golgi α-mannosidase from *Drosophila melanogaster*, one Jack bean α-mannosidase from *Canavalia ensiformis* and one not related.

I-Tasser generates five hit models using the templates above mentioned and the one with the best C-score (confidence) was chose to proceed in protocol. Lysosomal was predicted with more confidence than Golgi, due to a more successful alignment identity with other proteins. The new generated enzymes were subjected to relaxation by MD simulation for 20 ns, allowing the equilibration of atomic positions to a most stable structure in comparison with the model. After this, the models are ready for subsequent studies and analysis.

The 3D structures predicted for the proteins addressed in this study are shown in **Fig. 2** (A and D). Also was calculated the electrostatic potential surface of each enzymes with APBS-PDB2PQR server [12] and visual analysis was done. The hGMII (1144 amino acids) are bigger than hLM (1011 amino acids), the active center of hGMII larger and carring much negative charge in comparison with hLM. These facts contribute to a rational design of new compound for selective inhibition of hGMII.

To compare the models with the experimental solved structures, BLAST [13] alignment was used. The hGMII presents 43% of identity with 3blb, the mannosidase from drosophila, and hLM reveals an identification around 81% with the lysosomal mannosidase from bovine species.

Importantly, if the active sites were compared by sequence alignment, selecting only the amino acids present in this region, a very similar active site is identified, as showed in **fig. 1.** However small changes in amino acids, could lead to significant difference in interaction pattern and overall shape of active center, being importantly to study the compounds library in both cases: experimental structures and model ones.

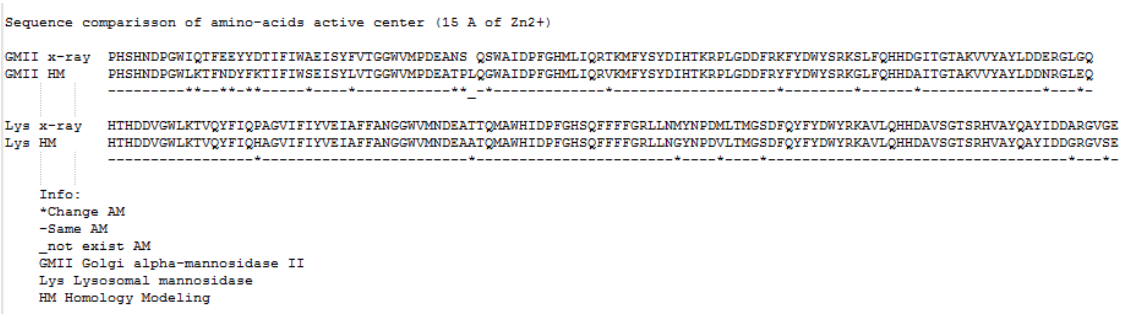

Fig. 1. Comparative analysis of active centers X-ray vs Homology Modeling structures

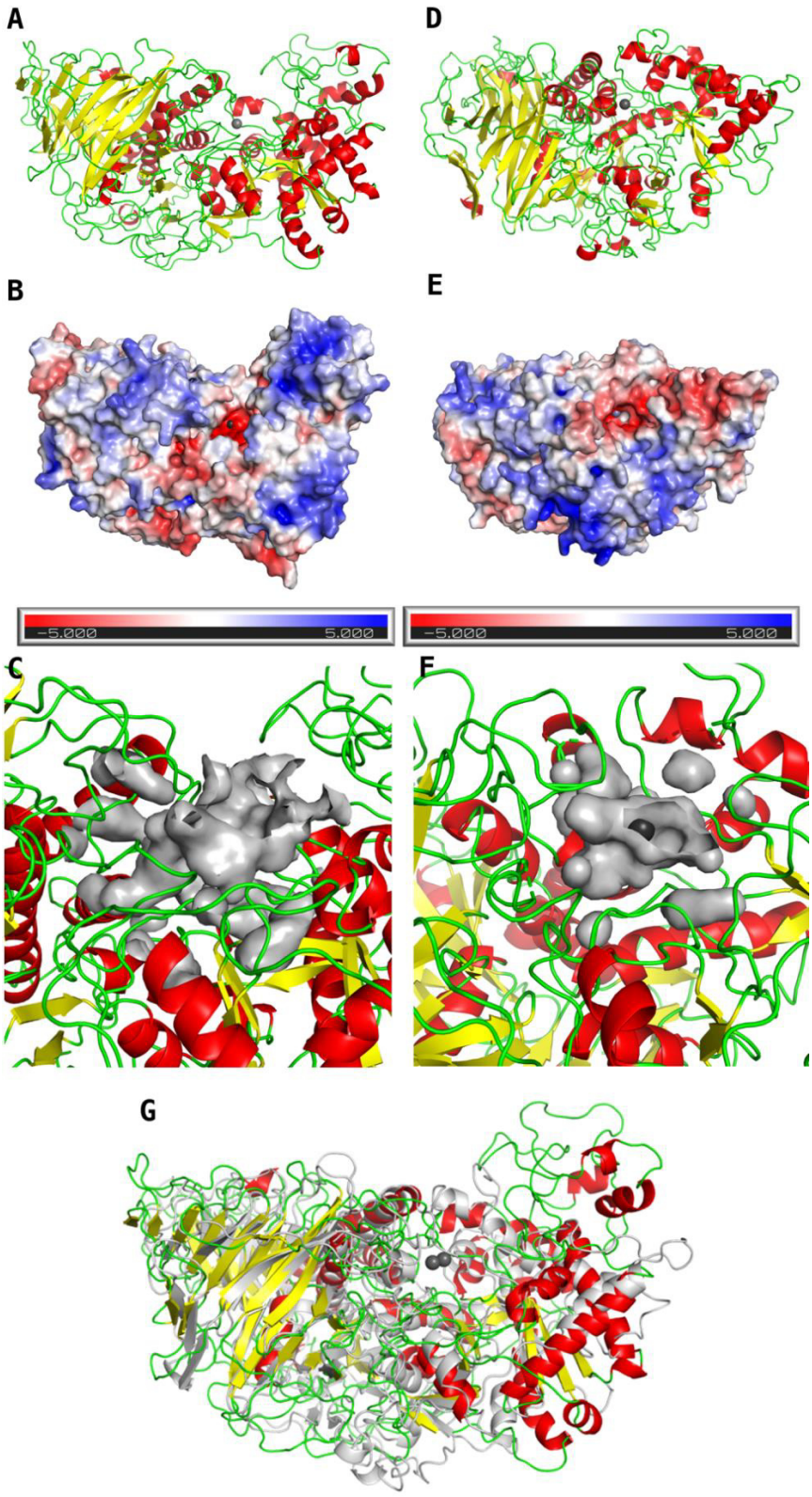

Fig. 2. (A-C) refer to the predicted structure of human Golgi α-mannosidase, where B shows the electrostatic potential surface and C highlights the active center pocket. (D-F) refer to the predicted structure of human lysosomal a-mannosidase, where E shows the electrostatic potential surface and F highlights the active center pocket. In the electrostatic potential surfaces, red represents the negative potential values and blue, the positive potential values; these potentials (k_b T e_c^{-1}) were calculated using APBS-PDB2PQR. The pockets present their cavities in grey surface representation. G shows the structure of human lysosomal a-mannosidase (light grey) superimposed to human Golgi α-mannosidase.

2.2.2 Ligand design and preparation

The design of new compounds were made by the following criteria: 1) hexahydropyrroloquinoline-2,3-diol (HHPQ) core was maintained; 2) modifications at positions 4 and 5 that can be substituted in synthetic process though electron demand Diels-Alder reaction or transformed after; 3) modification of aromatic ring substituents; 4) reactions viabilities; 5) reagents availabilities. Following this rational, 119 structures were designed. Before the docking studies, these structures were subjected optimization through DFT [14] calculations for obtention of a minimum Gibbs free energy by using Gaussian09 [15], with B3LYP function [16–20] and 6-31+G(d,p) [21–24] as basis set.

The optimized structures were transferred to pdbqt format (atomic coordinates, partial charges and AutoDock atom types), using OpenBabel [25] software, for the use on docking protocol.

2.2.3 Molecular docking studies: AutoDock Vina

The 119 optimized structures were submitted virtual screening by using AutoDock Vina [26] into experimental and model structures of Golgi and lysosomal mannosidases. The grid box was restricted to active center of enzyme and exhaustiveness option equal 40.

From the best $\Delta G_{binding}$, was calculated the energetic binding difference between X-ray structures (Golgi vs. lysosomal) and homology modeling structures. After that, were selected inhibitors more negative in at least -1.5 kcal/mol for Golgi. The **table 1** shows these differences, named $\Delta G_{affinity}$, and in supporting information all $\Delta G_{binding}$ are listed for the 119 molecules in all target enzymes.

Table 1. Selection of the best Docking Vina results, for GMII and LM X-ray structures

Analogue	ΔGaffinity	Analogue	ΔGaffinity	Analogue	ΔGaffinity	Analogue	ΔGaffinity
1	-2.8	**65**	-1.8	**41**	-1.6	**80**	-1.5
2	-2.3	**66**	-1.8	**95**	-1.6	**88**	-1.5
91	-2.1	**117**	-1.8	**39**	-1.6	**94**	-1.5
113	-2.0	**69**	-1.7	**11**	-1.5	**114**	-1.5
3	-1.8	**55**	-1.7	**40**	-1.5		

Analyzing the vina energies was observed that with R_5=pyrrolidone and R_3=acid result in affinity to Golgi α-mannosidase II, but if R_3 pass to methyl ester group, the affinity and the binding energy decrease. Also, more bulked esters did not demonstrate better results, as could be expected due the large active pocket for Golgi in comparison with lysosomal.

To perceive better this observations, image of docking positions was generated for the most negative binding energies, as seen in **fig. 3**. In additional **scheme 2** helps to fallow the inhibitors structures.

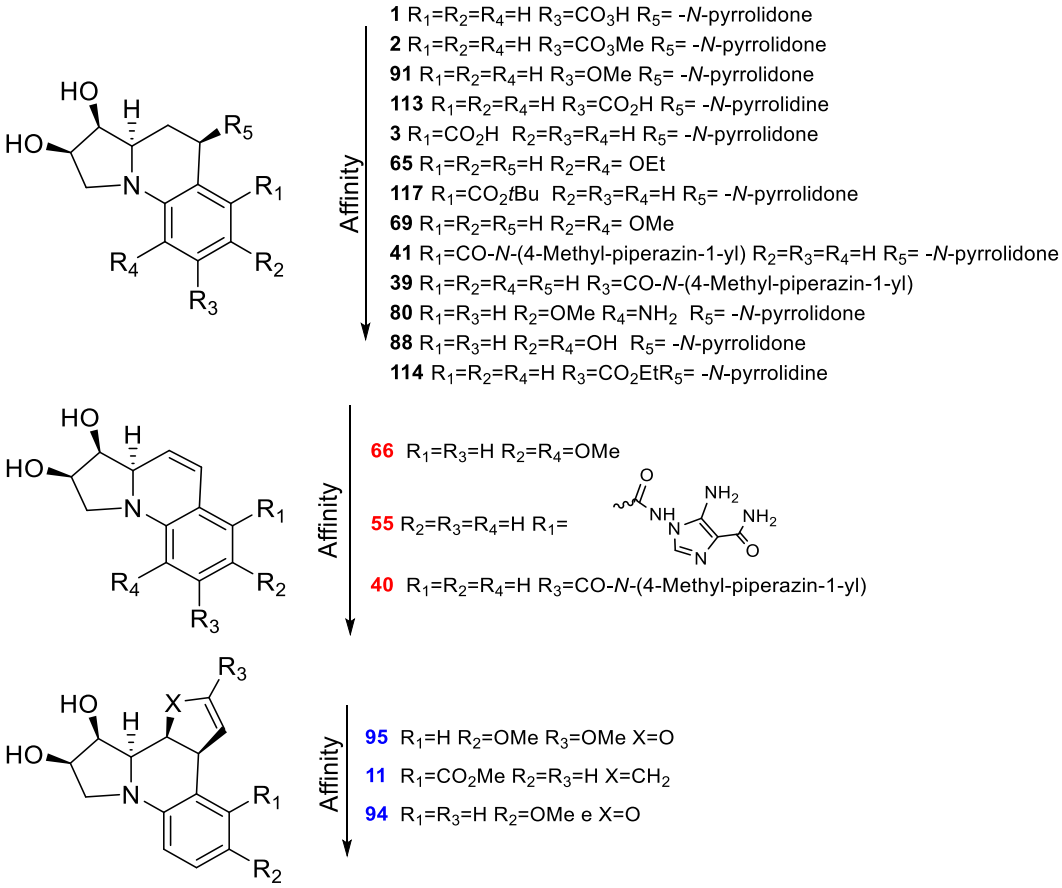

Scheme 2. Structures with the best results of vina for X-ray structures

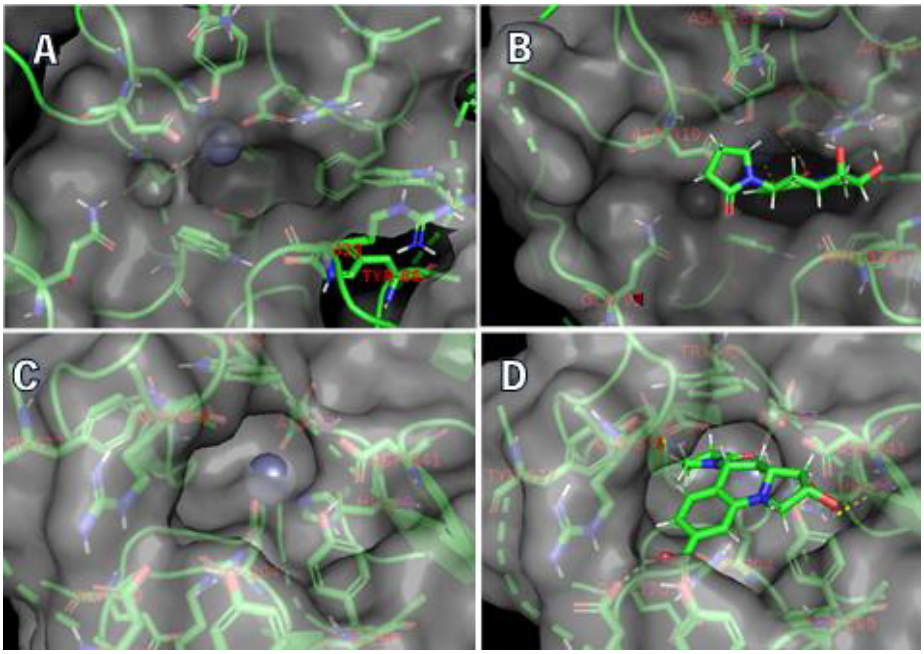

Fig. 3. A: Active center pocket of GMII X-ray B: Active center pocket of GMII X-ray with analogue **1**, C: Active center pocket of lysosomal X-ray D: Active center pocket of lysosomal X-ray with analogue **1**

Similarly, the virtual screening of the 119 structures was performed using the human models as target macromolecules, and results summarized in **table 2** and **scheme 3**.

Table 2. Vina $\Delta G_{affinity}$ results in homology modeling structures

Analogues	$\Delta G_{affinity}$	Analogues	$\Delta G_{affinity}$	Analogues	$\Delta G_{affinity}$
75	-2,2	**6**	-1,8	**31**	-1,5
46	-2,1	**39**	-1,7	**51**	-1,5
71	-2,0	**40**	-1,6		
118	-2,0	**44**	-1,6		
45	-2,0	**111**	-1,5		

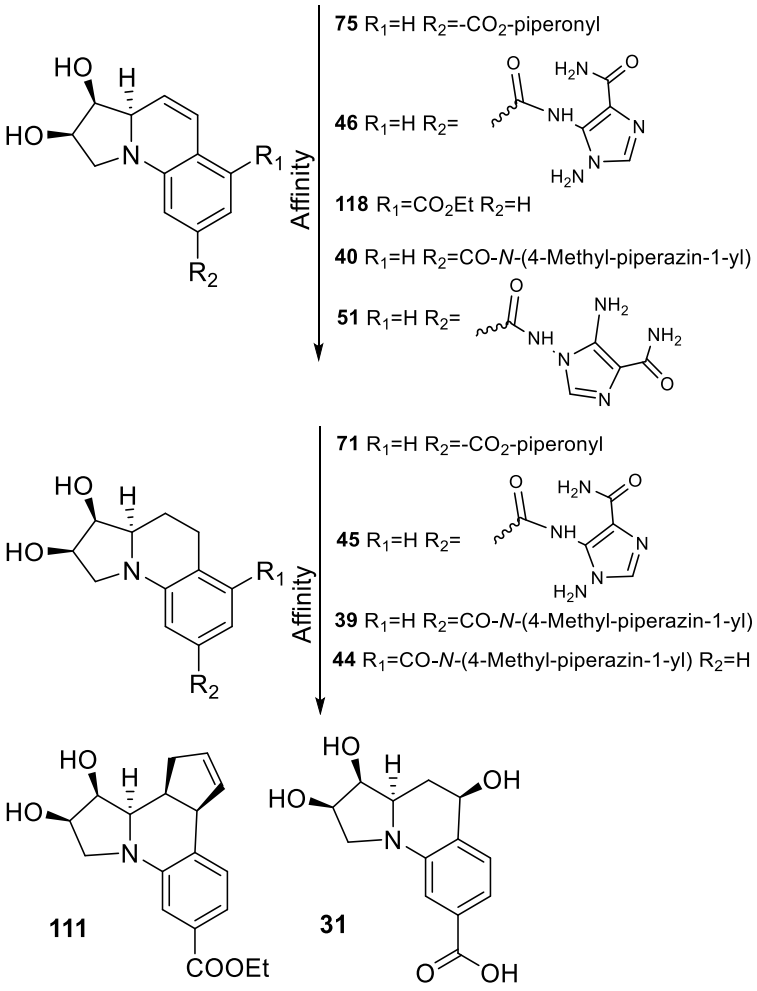

Scheme 3. Best results of vina docking for homology modeling structures

The hit results obtained for the human models were different than the observed for X-ray targets. This was expected, especially for Golgi, since some amino acids in the sequence vary between the organisms, also the binding pocket arrangement and interactions. As the goal of this work is to develop novel inhibitors selective for human Golgi α-mannosidase, the inhibitors with

best results in this target were selected to further analysis and studies. Therefore, the docking experiments using crystalline structures served more to solidify the use of the method and for comparative terms than to pursue the main objectives of the study.

Fig. 4 highlights the active pocket differences between the human models and also the binding mode of analog **75**, the one with best binding energy, using vina. These docking poses are a first indicative of selectivity of compound **75** towards hGMII, as the hydroxyl groups are near the Zn^{2+} in this case (**Fig. 4 B**) and more far in lysosomal active center (**Fig. 4 D**).

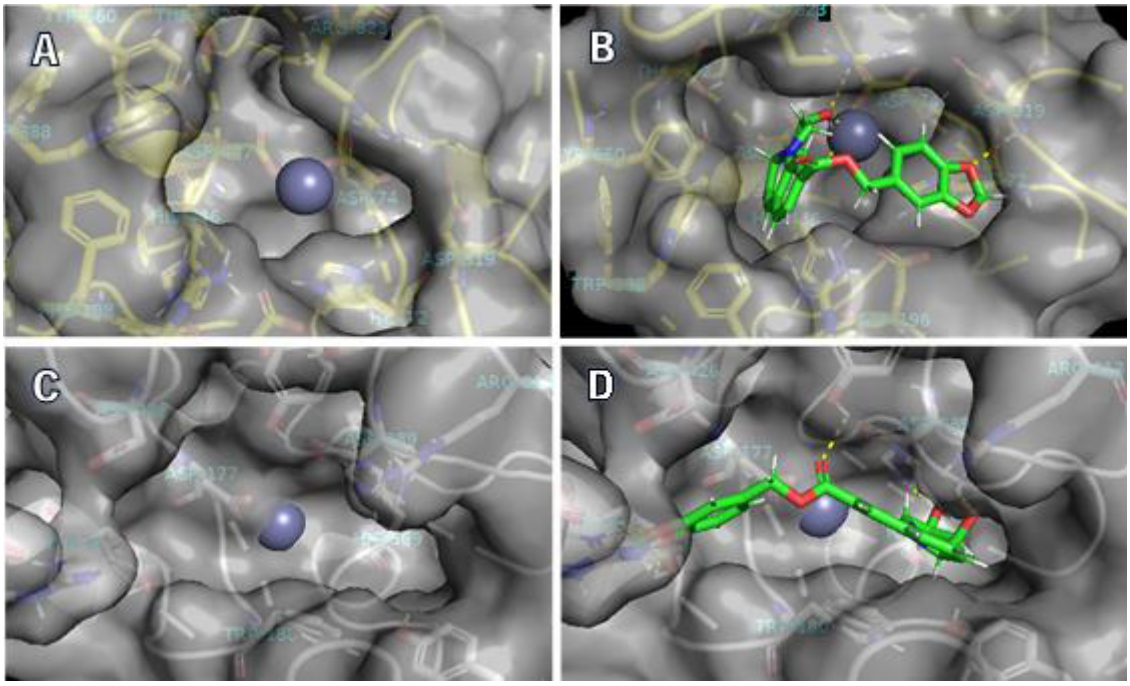

Fig. 4. A: Active pocket hGMII. B: Complex of hGMII with analogue **75** C: Active pocket hLM. D: Complex of hLM with analogue **75**

2.2.4 Molecular docking studies: AutoDock4 Zn

From the best results obtained with AutoDock Vina, for inhibitors in homology modelling structures, AutoDock 4 [27] was tested for method comparison. Twelve molecules were selected, and all of them demonstrated the same profile observed in vina, to binding with a more negative energy in Golgi α-mannosidase, however with less difference between the enzymes.

Analyzing case by case, the results were non-concordant with AutoDock Vina, as the same binding energy trend was not observed among the compounds. To fend off this problem, was decided to use optimized forcefield for zinc (AutoDock4 Zn). This method includes a potential able to describe the interactions of zinc with coordination ligands [28].

Using AutoDock4 Zn, the results of affinity were more concordant with vina results, despite the fact of vina not consider the zinc charge and contribution to the binding. **Table 3** list the binding energy difference ($\Delta G_{affinity}$) between hGMII *vs.* hLM.

Some known limitations of docking experiments refer to the fact that the proteins are static in this method, and only the ligand has movement, flexibility and torsions. In addition, solvation or desolvation are poor estimated as no explicit waters is present in docking. Because of that, it is reasonable to use MD simulations to make end point decisions. Five compounds were selected (**Fig. 5**) for future evaluation using MD simulations, respecting the criteria: 1) reject very much similar structures 2) select compounds by simple and viable pathway synthesis.

Table 3. Result of $\Delta G_{affinity}$ using AutoDock4 Zn and human mannosidase models

Analogue	$\Delta G_{affinity}$	Analogue	$\Delta G_{affinity}$	Analogue	$\Delta G_{affinity}$
118	-3,92	46	-1,39	**75**	-0,18
51	-2,12	**39**	-1,35	44	3,20
6	-2,09	40	-1,18		
71	-2,07	**111**	-1,05		
31	-1,55	45	-0,52		

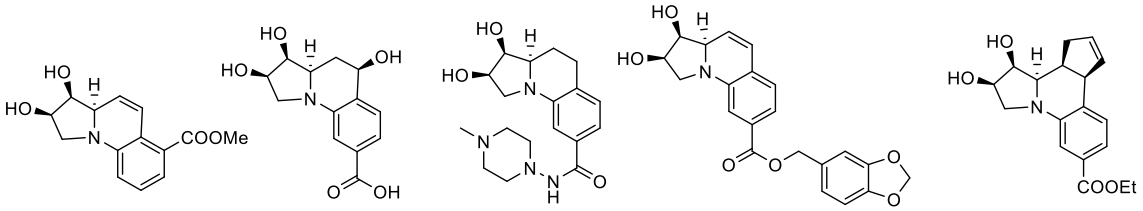

6 **31** **39** **75** **111**

Fig. 5. Structures of the selected compounds for MD studies, in complex to hGMII and hLM

2.2.5 Molecular dynamics studies

From AutoDock4 Zn docking poses, MD simulations of the 5 complexes for each enzyme were carried out during 10 ns. This was done to perceive the stability of each complex, to see the compound behavior in active center and the interaction with amino acids. All compounds stay at active center during the simulation. However more deep analysis allows to make some conclusions without prolongating the simulation time, which request huge computing resource and time.

First, was followed the RMSD (Root Mean Square Deviation) analysis, which is a measure of the deviation of the particles position with respect to a reference structure over time. For this calculation was chosen the amino acids of active center in the presence of the selected

compounds, which give us the relative stability of the active center when a ligand is bound. The results demonstrate that in the presence of compound **31** hGMII are more stable than hLM, next compound **75**. Oppositely, these two compounds induce a considerable change at hLM active center.

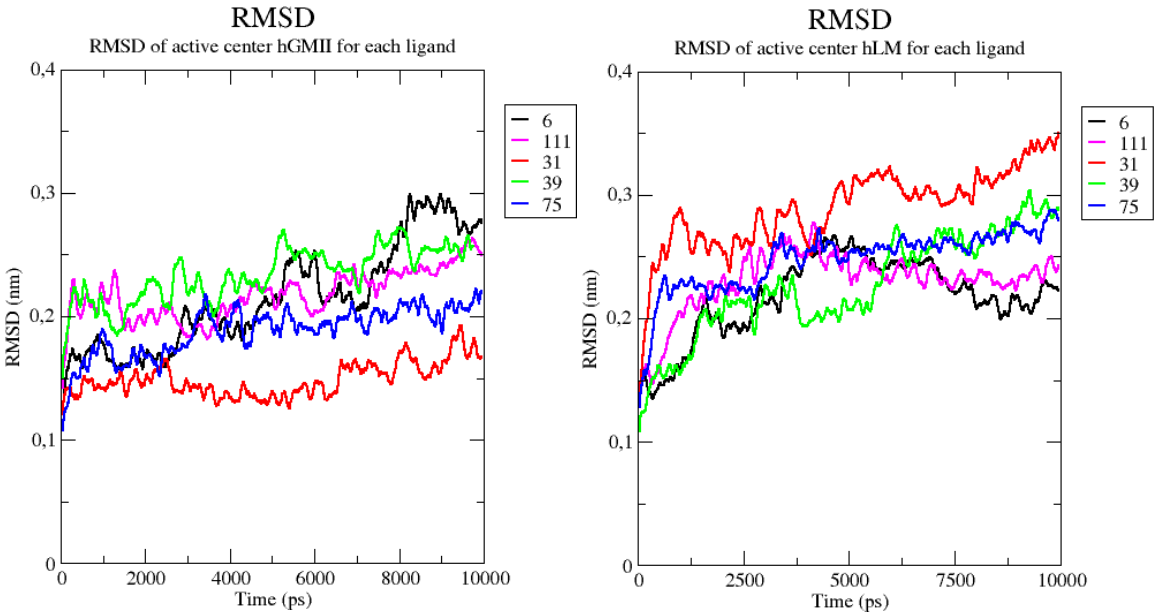

Graphic 1. RMSD analysis of active center in presence of ligand for hGMII (left) and hLM (right)

Several analyses, as RMSF, Hydrogen Bond and distance between Zn^{2+} and ligands, were performed. However, these results were not useful to distinguish a selectivity towards Golgi mannosidase. In this sense, was calculated the middle conformation of the ligand during the last 5 ns of simulations, where complexes were stabilized. This is done using the clustering analysis, which can find out the most representative structure of the inhibitor, in a time interval, resulting in a conformation for visual evaluation, *i.e.* will tell the most sampled position of the compounds in active site (**Fig. 6**).

The conformation generated in this analysis helps to understand the proximity of HHPQ ring and hydroxyl groups to the Zn^{2+} ion, which proves to be more comparative among the systems than other analysis tested.

Comparing the compound position in both active sites (**Fig. 6**), some interesting conclusions emerge. Compound **6** positioned its hydroxyl group in similar way (near zinc) in the two enzymes, while **39** is far from zinc ion in both cases. For the ligand **111** the most sampled conformation in the two enzymes does not help to distinguish a preferred binding. Finally, inhibitors **31** and **75** are the two cases where we can infer a selectivity towards Golgi, as the HHPQ core is oriented and the diol very near to zinc ion, for these compounds. This arrangement is very different of the ones sampled in lysosomal.

2.3 Conclusions

For this study different molecular modelling techniques were implemented, from structure prediction to molecular dynamics, to address the binding of novel inhibitors to mannosidases. Currently, most studies addressing the activity of inhibitors in Golgi and lysosomal mannosidases, make use of structures from another organism, not human. That is why understand in detail the structure and interactions in human Golgi mannosidase is very important to best design novel selective inhibitors.

The results show that despite the conserved similarity to mannosidases from other species, the activity pocket of the human models is different. Importantly, the pocket in Golgi is more opened than in lysosomal, indicating that one possible strategy would be increase the size and volume of the inhibitor compound.

Docking experiments were a first attempt to design and chose selective ligands. With this technique a library of 119 compounds was screened against the enzymes and 5 hit structures were selected.

Molecular dynamics simulations evaluated the stability of the complexes from the best five docking results, trying to better differentiate the affinity to both enzymes. From the complete computational protocol, only 2 ligands demonstrated selectivity towards Golgi, the compounds **31** and **75**.

Simulating the complexes for mores nanoseconds could distinguish and give more information about the evaluated systems. These enzymes comprising a high number of amino acids, making these systems very computational demanding and time consuming.

We highlight that the findings we obtained suggest lead compounds to synthesis and further biological studies. Importantly, novel molecules could be designed using the top 5 structures.

Acknowledge

"Search-ON2: Revitalization of HPC infrastructure of UMinho, (NORTE-07-0162-FEDER-000086), co-funded by the North Portugal Regional Operational Programme (ON.2-O Novo Norte), under the National Strategic Reference Framework (NSRF), through the European Regional Development Fund (ERDF).

Supporting Information (optimized structures list, docking energies, enzyme models) available at attached file.

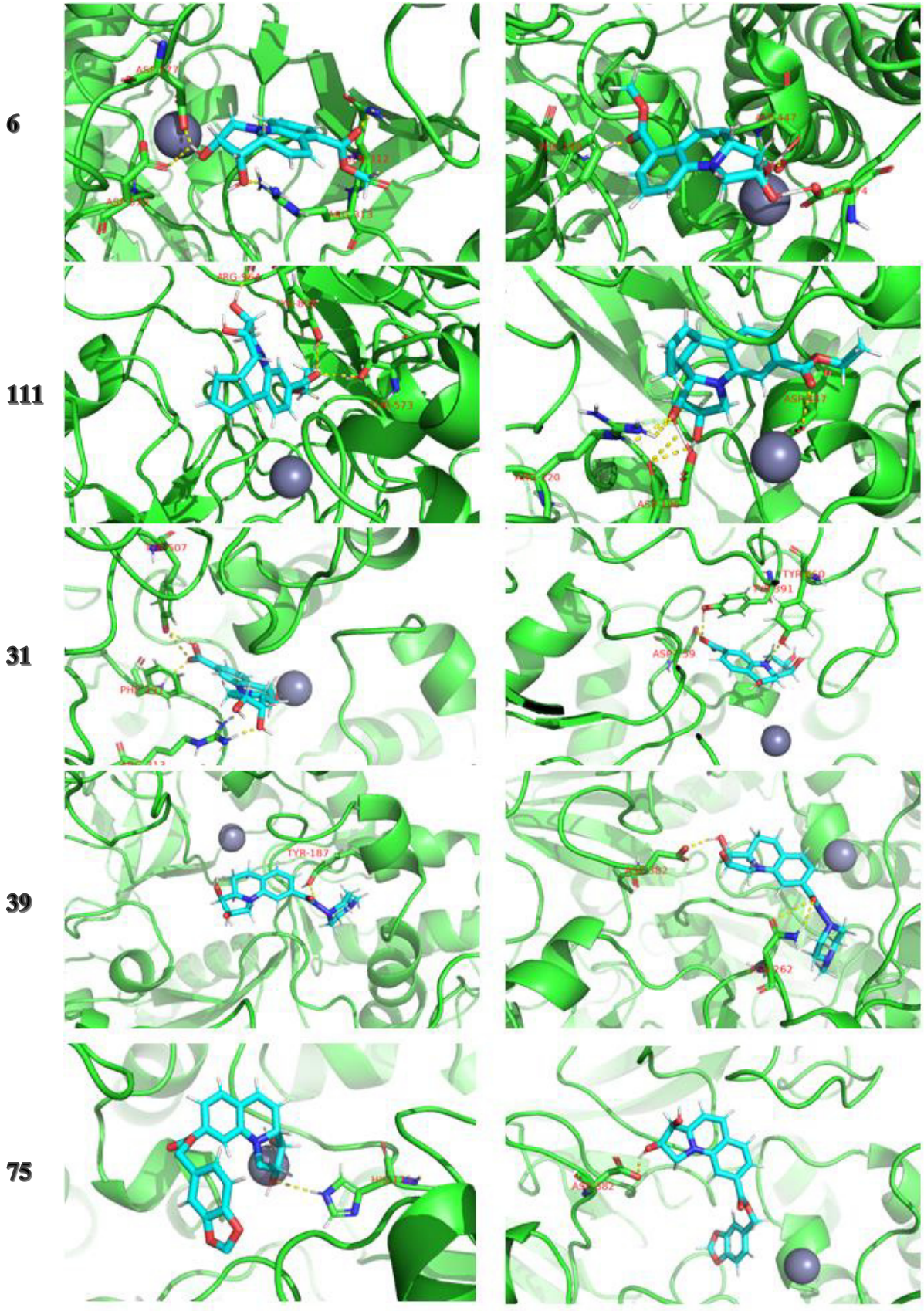

Fig. 6. Abundant of ligands position after last 5 ns of MM simulation complexes of hGMII (left) and hLM (right) with interaction by hydrogen bond with amino acid of enzyme

2.4 Molecular modelling options

2.4.1 Molecular docking

Docking experiments were performed with Vina, AutoDock 4.0 and AutoDock Zn and prepared with the AutoDock tools software. As macromolecules, X-ray structures of Golgi and lysosomal were used, as above mentioned, and the most representative structures from MD equilibration of human models.

In the case of vina, this method has a simpler implementation, using a combination of scoring function and an optimization algorithm, being fastest in predict docking poses. For this method a grid spacing of 1 Å is used, therefore the grid points, *i.e.*, the size of the box where the search is done, vary accordingly the enzyme and inhibitors, but the box is always centered at the zinc ion. An exhaustiveness of 40 and num_modes = 5 were used.

For AutoDock 4 or AutoDock 4 Zn, Lamarckian genetic algorithm (LGA) was chosen as search algorithm. Similarly, a grid box was created and centered near Zn ion, but in a resolution of 0.375 Å, with the necessary size to involve all inhibitors sizes/volume. Grid potential maps were calculated using AutoGrid 4.0. Each docking consisted of 50 independent runs, with a population of 150 individuals, a maximum number of $25x10^6$ energy evaluations and a maximum number of 27,000 generations.

2.4.2 Molecular dynamics simulations

All simulations were performed using the GROMACS 5.1.4 version [29], within the GROMOS 54a7 force field (FF) [30].

The first simulations were carried out to equilibrate the human models generated *via* PSP method. Both enzymes were modeled in water with the simple point charge (SPC) water model in a cubic box with a hydration layer of at least 1.5 nm between the macromolecule and the walls.

To achieve system neutrality counter ions were added to the simulation boxes. One stage of energy minimization was performed using a maximum of 50,000 steps with steepest descent algorithm for both structures. The systems were initialized in a NVT ensemble, using V-rescale algorithm [31], with the coupling constant τT = 0.10 ps, to control temperature at 310 K (37 °C). After that, a NPT initialization step was performed, with V-rescale and Parrinello-Rahman [32] barostat algorithms to couple temperature and pressure at 310 K and 1 atm respectively. Was used the following coupling constants: τ_T = 0.10 ps and τP = 2.0 ps. Position restraints (with force constant

of 1000 $kJ.mol^{-1}.nm^{2}$) were applied to all protein heavy atoms in initialization steps. 20 ns of MD simulations were performed for each system, without position restraints, and with the same NPT ensemble described above. The Lennard-Jones interactions were truncated at 1.4 nm and using particle-mesh Ewald (PME) method for electrostatic interactions, also with a cut-off of 1.4 nm. The algorithm LINCS was used to constrain the chemical bonds of the peptides and the algorithm SETTLE was used in the case of water.

The second type of simulation were performed using the best docking pose for the 5 selected cases in each human enzyme model. These simulations were performed during 10 ns, to perceive the spontaneous tendency of the inhibitor to remain or leave the active center, or simply to observe the interaction pattern with the target or the conformational changes which causes to the enzymes.

To simulate the complex, it is necessary to generate GROMOS parameters for the inhibitors molecules using ATB [33], making these compounds recognizable by the Force Field. These simulations followed the above described parameters.

2.4.3 Analysis

For visual analysis and take pictures was used PyMOL [34]. Other analyses were performed using the tools available in GROMACS.

The analysis RMSD or root mean square deviation is very used in this field, to follow the conformational changes along time, in comparison with a reference structure. For this study, the active center was the focus, where we calculated the deviations in the presence of a ligand.

The clustering analysis minimize the RMSD variance and results in a conformation that best represents all the frames sampled, being possible to see the most probable arrange of the inhibitor at the active site.

Hydrogen bonds were followed through PyMOL, to see the interaction pattern among the inhibitors and enzymes. Other analyses, as RMSF and distance were performed for the complexes, but were not helpful to distinguish the systems.

2.5 References

(1) Bols, M.; Lopez, O.; Ortega-Caballero, F. *Comprehensive Glycoscience*; Kamerling, H., Ed.; Elsevier Science, 2007. https://doi.org/10.1016/B978-044451967-2/00100-8.

(2) Legler, G. *Glycosidase Inhibition by Basic Sugar Analogs and the Transition State of Enzymatic Glycoside Hydrolysis*; Univ.-Prof. Dipl.-Ing. Dr. Arnold E. Stütz, Ed.; 1998. https://doi.org/10.1002/3527601740.ch3.

(3) Gross, P. E.; Baker, M. A.; Carver, J. P.; Dennis, J. W. Inhibitors of Carbohydrate Processing: A New Class of

Anticancer Agents. *Clin Cancer Res.* **1995**, *1* (9), 935–944.
(4) Fuhrmann, U.; Bause, E.; Legler, G.; Ploegh, H. Novel Mannosidase Inhibitor Blocking Conversion of High Mannose to Complex Oligosaccharides. *Nature* **1984**, *307*, 755–758. https://doi.org/10.1038/307755a0.
(5) Snith, S. M.; Levvy, G. A. α-Mannosidase as a Zinc-Dependent Enzyme. *Nature* **1968**, *218*, 91–92. https://doi.org/10.1038/218091a0.
(6) Elsen, J. M. H. Van Den; Kuntz, D. A.; Rose, D. R. Structure of Golgi a -Mannosidase II : A Target for Inhibition of Growth and Metastasis of Cancer Cells. *Euro. Mol. Biol. Org.* **2001**, *20* (12), 3008–3. https://doi.org/10.1093/emboj/20.12.3008.
(7) Zhang, Y. I-TASSER Server for Protein 3D Structure Prediction. *BMC Bioinformatics* **2008**, *9* (40). https://doi.org/10.1186/1471-2105-9-40.
(8) Roy, A.; Kucukural, A.; Zhang, Y. I-TASSER: A Unified Platform for Automated Protein Structure and Function Prediction. *Nat. Protoc.* **2010**, *5*, 725–738. https://doi.org/10.1038/nprot.2010.5.
(9) Yang, J.; Yan, R.; Roy, A.; Xu, D.; Poisson, J.; Zhang, Y. The I-TASSER Suite: Protein Structure and Function Prediction. *Nat. Methods* **2015**, *12* (1), 7–8. https://doi.org/10.1038/nmeth.3213.
(10) Berman, H. M.; Westbrook, J.; Feng, Z.; Gilliland, G.; Bhat, T. N.; Weissig, H.; Shindyalov, I. N.; Bourne, P. E. The Protein Data Bank. *Nucleic Acids Res.* **2000**, *28* (1), 235–242. https://doi.org/10.1093/nar/28.1.235.
(11) Consortium, T. U. UniProt: A Worldwide Hub of Protein Knowledge. *Nucleic Acids Res.* **2018**, *47* (D1), D506–D515. https://doi.org/10.1093/nar/gky1049.
(12) Jurrus, E.; Engel, D.; Star, K.; Monson, K.; Brandi, J.; Felberg, L. E.; Brookes, D. H.; Wilson, L.; Chen, J.; Liles, K.; et al. Improvements to the APBS Biomolecular Solvation Software Suite. *Protein Sci.* **2018**, *27*, 112–128. https://doi.org/10.1002/pro.3280.
(13) Altschul, S. F.; Gish, W.; Miller, W.; Myers, E. W.; Lipman, D. J. Basic Local Alignment Search Tool. *J. Mol. Biol* **1990**, *215*, 403–410. https://doi.org/10.1016/S0022-2836(05)80360-2.
(14) Hohenberg, P. .; Kohn, W. Inhomogeneous Electron Gas. *Phys. Rev.* **1964**, 136 (3b), B864.
(15) Frisch, M. J. .; Trucks, G. W. .; Schlegel, H. B. .; Scuseria, G. E. .; Robb, M. A. .; Cheeseman, J. R. .; Scalmani, G. .; Barone, V. .; Mennucci, B. .; Petersson, G. A. .; et al. Gaussian09. Gaussian, Inc: Wallingford, CT, USA 2009.
(16) Becke, A. D. A New Mixing of Hartree-Fock and Local Density-functional Theories. *J. Chem. Phys.* **1993**, *92* (2), 1372–1377.
(17) Becke, A. D. Density-Functional Thermochemistry. III. The Role of Exact Exchange. *J. Chem. Phys.* **1993**, *98* (7), 5648–5652.
(18) Lee, C. T. .; Yang, W. T. .; Parr, R. G. Development of the Colle-Salvetti Correlation-Energy Formula into a Functional of the Electron Density. *Condens. Matter Mater. Phys* **1988**, *37* (2), 785–789.
(19) Vosko, S. H. .; Wilk, L. .; Nusair, M. Accurate Spin-Dependent Electron Liquid Correlation Energies for Local Spin Density Calculations: A Critical Analysis. *Can. J. Phys* **1980**, *58* (8), 1200–1211.
(20) Stephens, P. J. .; Devlin, F. J. .; Chabalowski, C. F. .; Frisch, M. J. Ab Initio Calculation of Vibrational Absorption and Circular Dichroism Spectra Using Density Functional Force Fields. *J. Phys. Chem.* **1994**, *98* (45), 11623–11627.
(21) Rassolov, V. A. .; Ratner, M. A. .; Pople, J. A. .; Redfern, P. C. .; Curtiss, L. 6-31G* Basis Set for Third-Row Atoms. *J. Comput. Chem.* **2001**, *22* (9), 976–984.
(22) Ditchfield, R. .; Hehre, W. J. .; Pople, J. A. Self-Consistent Molecular-Orbital Methods. IX. An Extended Gaussian-Type Basis for Molecular-Orbital Studies of Organic Molecules. *J. Chem. Phys.* **1971**, *54* (2), 724.
(23) Hariharan, P. C. .; Pople, J. A. Accuracy of AH n Equilibrium Geometries by Single Determinant Molecular Orbital Theory. *Mol. Phys* **1974**, *27* (1), 209–214.
(24) Gordon, M. S. The Isomers of Silacyclopropane. *Chem. Phys. Lett.* **1980**, *76* (1), 163–168.
(25) O'Boyle, N. M.; Banck, M.; James, C. A.; Morley, C.; Vandermeersch, T.; Hutchison, G. R. Open Babel: An Open Chemical Toolbox. *J. Cheminform.* **2011**, *3* (1), 33. https://doi.org/10.1186/1758-2946-3-33.
(26) Trott, O.; Olson, A. J. AutoDock Vina: Improving the Speed and Accuracy of Docking with a New Scoring Function, Efficient Optimization and Multithreading. *J. Comput. Chem.* **2010**, *31*, 455–461.
(27) Morris, G. M.; Huey, R.; Lindstrom, W.; Sanner, M. F.; Belew, R. K.; Goodsell, D. S.; Olson, A. J. Autodock4 and AutoDockTools4: Automated Docking with Selective Receptor Flexiblity. *J. Comput. Chem.* **2009**, *16*, 2785–2791.
(28) Santos-Martins, D.; Forli, S.; Ramos, M. J.; J., O. A. AutoDock4(Zn): An Improved AutoDock Force Field for Small-Molecule Docking to Zinc Metalloproteins. *J Chem Inf Model* **2014**, *54* (8), 2371–2379. https://doi.org/10.1021/ci500209e.
(29) Spoel, D. Van Der; Lindahl, E.; Hess, B.; Groenhof, G.; Mark, A. E.; Berendsen, H. J. C. GROMACS: Fast, Flexible, and Free. *J. Comput. Chem.* **2005**, *26* (16), 1701–1718. https://doi.org/10.1002/jcc.20291.

(30) Schuler, L. D.; Daura, X.; van Gunsteren, W. F. An Improved GROMOS96 Force Field for Aliphatic Hydrocarbons in the Condensed Phase. *J. Comput. Chem.* **2001**, *22* (11), 1205–1218. https://doi.org/10.1002/jcc.1078.
(31) Bussi, G.; Donadio, D.; Parrinello, M. Canonical Sampling through Velocity Rescaling. *J. Chem. Phys.* **2007**, *126* (1), 14101. https://doi.org/10.1063/1.2408420.
(32) Martoňák, R.; Laio, A.; Parrinello, M. Predicting Crystal Structures: The Parrinello-Rahman Method Revisited. *Phys. Rev. Lett.* **2003**, *90* (7), 4. https://doi.org/10.1103/PhysRevLett.90.075503.
(33) Malde, A.K.; Zuo, L.; Breeze, M.; Stroet, M.; Poger, D.; Nair, P. C.; Oostenbrink, C.; Mark, A. E. An Automated Force Field Topology Builder (ATB) and Repository: Version 1.0. *J. Chem. Theory Comput.* **2011**, *7* (12), 4026–4037. https://doi.org/10.1021/ct200196m.
(34) The PyMOL Molecular Graphics System, Version 2.2.2 Schrödinger, LLC.

Chapter III: Results and discussion. Experimental work.

"Chemistry begins in the stars. The stars are the source of the chemical elements, which are the building blocks of matter and the core of our subject."

Peter Atkins

3.1 Introduction

Tetrahydroquinoline (THQ) or 1,2,3,4-tetrahydroquinoline is an important framework to which a variety of biological activities are ascribed. This core-structure is present in natural products, and plays a key role in synthesis of new drugs in pharmaceutical industry. Natural products range from simple alkyl derivatives to more elaborated polycyclic structures. *E.g.* 2-methyl-THQ is present in human brain; 2-arylalkyl: (-)-angustureine, (**1**) (-)-cuspareine, (-)-galipeine (**2**) isolated from a Venezuelan shrub-like tree display a variety of medicinal properties[1,2]. Synthetic 1,2,3,4-THQs derivatives have been design to meet an array of biological applications, from cardiovascular agents, to anticancer agents, immunosuppressors, antiplasmodial. For example oxamniquine (**3**), sold under the brand name Vansil, treat schistosomiasis; THQ L-689,560 (**4**) is a potent antagonist at the glycine-NMDA receptor [3].

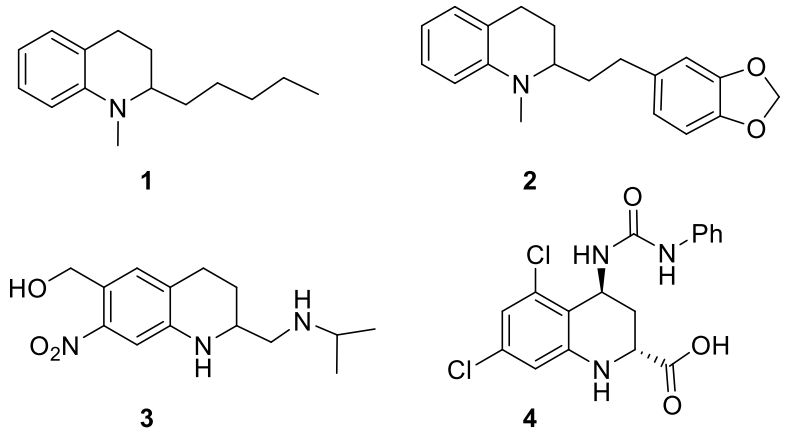

Fig. 3. THQs of natural sources: angustureine (**1**), galipeine (**2**); synthetic THQs: oxamniquine (**2**), L-689,560 (**4**)

Besides, pharmacological applications, THQ derivatives have also other important applications as pesticides, corrosion inhibitors, and antioxidants. Some THQ have been used as coordination ligands with various metals, such as rhodium and iridium, in asymmetric synthesis [1].

THQs were previously synthetized in our laboratory by Povarov's reaction from protected D-erythrose (**5**) and *p*-anisidine [4] (**Scheme 1**). In this work were described the synthesis of other THQs starting from D-erythrose and other anilines. HHPQ were obtained from THQ by aminocyclization.

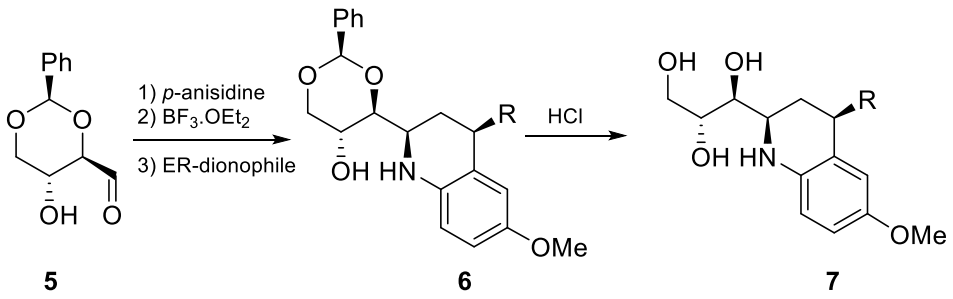

Scheme 1. Previous work of synthesis functionalized tetrahydroquinolines

3.2 Results and discussion

The main objective of this work is the synthesis of new THQs derived from reaction of anilines with aldehyde **5**, followed by *in situ* reaction of the imines with electron rich dienophiles, and further cyclization of THQs into HHPQ. The starting aldehyde **5**, was prepared from D-glucose according to the literature procedure [5–8], which includes a methodological upgrade with yield improvement and reaction scale-up (**Scheme 2**) [9]. Anilines substituted at *m*-position with esters groups were prepared according to the literature described for methyl ester [10], or by Fisher esterification from respective amino-acids followed by neutralization.

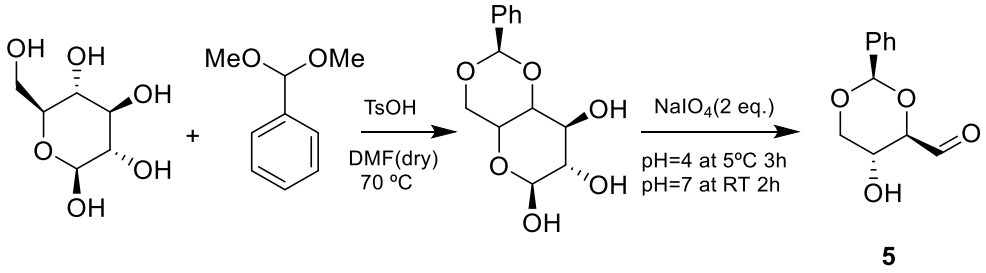

Scheme 2 Synthesis of the starting material, D-erythrose (**5**)

3.2.1 Synthesis of D-erythrosylimines

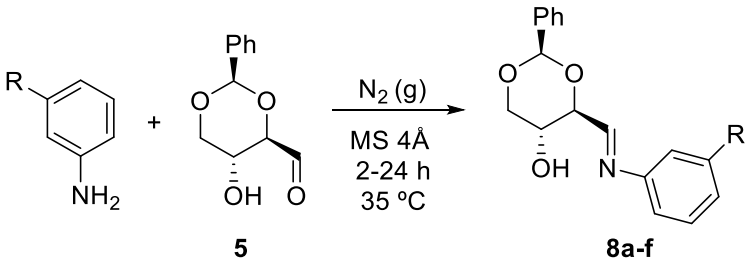

Entry	R	Time(h)
a	H	2
b	CO_2Me	1
c	CO_2Et	2
d	CO_2iPr	2
e	OH	24
f	OMe	24

Scheme 3. Synthesis of D-erythrosylimines (**8a-f**)

Imines **8** were prepared "*in situ*" by reaction of aldehyde **5** with aniline, anilines bearing electron-donating groups, and anilines bearing electron-withdrawing groups. Reactions were run in THF or ACN in the presence of MS 4 Å at 35 °C for 1-24 h (**Scheme 3**). The syntheses of aromatic imines containing *m*-EDG were completed in 24 hours. Reactions were much faster (1-2 hours) with anilines bearing *m*-EWG. The formed imines bearing EWG has to be used immediately after preparation. On the contrary imines with EDG are stable under the reaction conditions. Anilines bearing the carboxylic acid group do not react even after heating at 40 °C for 24 h.

3.2.2 Addition of *N*-vinyl pyrrolidone to *m*-substituted imines

The crude imines **8a-f** were subjected to inverse electron demand Diels-Alder cycloaddition (DA_{INV}) with *N*-vinylpyrrolidone. The imine reaction mixture previously made in the first step was cooled to -79 °C, BF_3.ether was added, followed by the dienophile. The temperature was then allowed to rise to reach room temperature for 2-19 h. The reaction of imine **8a** took run in ACN gave a better yield (52%) than the one run in THF, 34%. Reactions of aromatic imines bearing *m*-EWG **8b-d** took 2 hours to be completed. Reactions of imines incorporating *m*-EDGs did not occur, even prolonging the reaction period till 24 hours. ^{1}H NMR showed no signs of cycloadducts, but only degradation products (**Scheme 4**). The crude products were subjected to flash chromatography, giving inseparable mixtures of isomers **9** and **10** in ratio, and overall yields described in **Table 1** (from D-glyceraldehyde **5**).

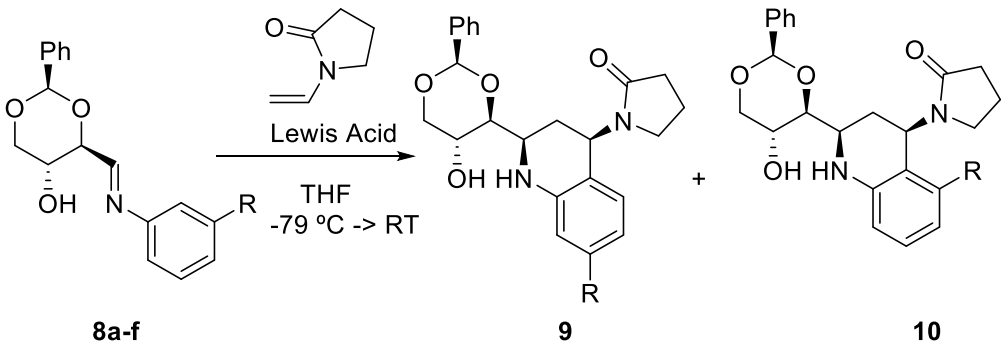

Scheme 4. Inverse electron demand Diels-Alder reaction of *m*-substituted imines with *N*-vinylpyrrolidone

Table 1. Yields and isomeric ratio of products obtained from inverse Diels-Alder cycloaddition. Yield from **5** (global); NR=not reacted; *from NMR spectra

R=	H	CO_2Me	CO_2Et	CO_2iPr	OH	OMe
Yield (%)	52	44	55	51	NR	NR
Ratio* (**9**/**10**)	1:1	0:1	0.7:1	0.4:1	x	x

The *regio*-seletivity directing effect of different alkyl group inserted into the ester function in the phenyl ring *m*-position was evaluated to see if the isomeric ratio of products **9** and **10** could be altered. With imine **8b** the reaction in THF demonstrated to be completely selective giving a single *regio*-isomer, **10** in 44% yield. The yield decreased to 32% when the reaction was run in ACN, and maintaining the *regio*-selectivity. Reactions of imines **8c**,**d** (in THF) containing bulkier alkyl groups (ethyl and isopropyl) were run to find if the "bottom" position of the aromatic ring could be preferred (compound **9**). The results showed that the ethyl group is able to induce a new *regio*-isomer, 0.7 (**9**) :1.0 (**10**) ratio. The introduction of a larger group, isopropyl, was expected to improve the isomeric ratio towards the isomer **9**, but in fact gave a 0.4:1.0, favored to the "top" position. This is not consistent with a simple steric effect. Chromatographic separations were tried in both cases but were found useless.

With the aim to modify the *regio*-preference of the reactions in order to obtain isomers **9**, a couple of bidentate Lewis acids were studied as catalysts in the cycloadditions, instead BF_3.ether. Imine **8c** was used as model (**Table 2**). A mixture of both isomers was formed in both cases: with $Ln(OTf)_3$ a 1:1 mixture of products **9c** and **10c** was formed, with a very low yield; with $InCl_3$ a 1:2 ratio of products is formed, but favoring **10c**.

Table 2. Evaluation of Lewis acid effect; Yield from **5** (global); *from ^{1}H NMR spectra

Lewis Acid	**$BF_3.OEt_2$**	**$InCl_3$**	**$Ln(OTf)_3$**
η_{global} (R=CO_2Et)	55%	40%	9%
Isomeric ratio* (**9c**:**10c**)	0.7:1	0.5:1	1:1

To guide the ester group into the "bottom" position of the structure, an *ortho-meta* substituted aniline was used (**Scheme 5**). Imine **11** was obtained in 2 hours, in THF and used in the next step without purification. Product **12** was obtained in 30% overall yield, as an amorphous solid.

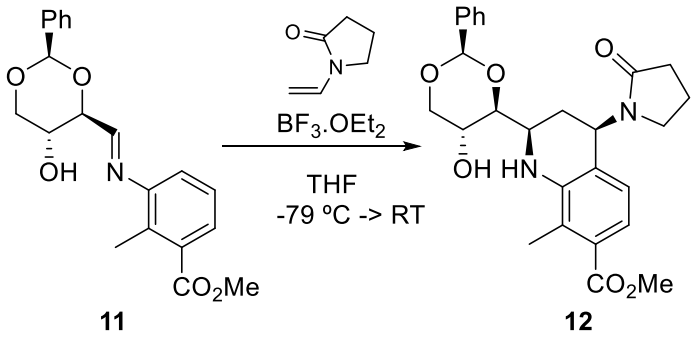

Scheme 5. Synthesis of THQ from *ortho-meta*-substituted imine.

3.2.3 Aminocyclization of THQ towards hexahydropyrroloquinoline.

Structure **13** compiles all the THQs obtained, which will be subjected to cyclization. First the acetal cleavage occurred under HCl with formation of the hydrolyzed THQs as ammonium salts **14a-d**. The benzaldehyde formed was evaporated. The cyclization of the triol chain into the THQ moiety with formation of HHPQ was tried under various strategies, which included transformation of terminal hydroxyl group into a good living group through mesylation or tosylation together with activation of the amino group with Cbz or Boc. All the trials fail giving many side products. The literature describes chlorination of hydroxyls, and epoxidation as possible [11].

An efficient cyclization was accomplished by an one-pot methodology: 1) bromination of primary alcohol under HBr in acetic acid for 1 hour; 2) addition of a large amount of methanol to

provide esterification of acetic acid into ethyl acetate which facilitate evaporation in the final step; 3) addition of solid Na_2CO_3 and a few drops of water to alkalinize the reaction medium promote aminocyclization to give HHPQ **15a-d**. Simple work-up as evaporation to dryness and liquid-solid extraction of the residue with DCM gave relatively pure products, cases **15b-d** (**Scheme 6**). Cyclization also occurred in the presence of TEA instead Na_2CO_3, giving products contaminated with triethyl ammonium salts, which result to be difficult to isolate by flash chromatography even under gradient elution.

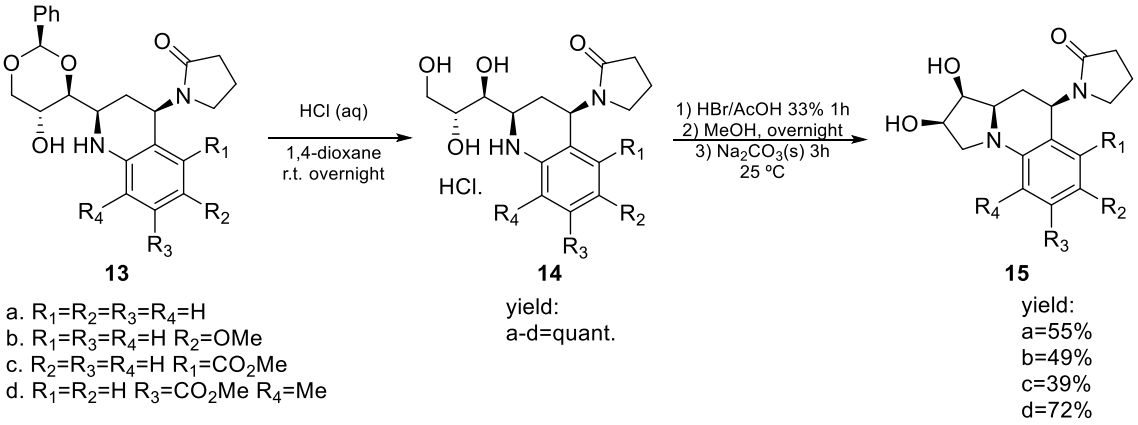

13

a. $R_1=R_2=R_3=R_4=H$
b. $R_1=R_3=R_4=H$ $R_2=OMe$
c. $R_2=R_3=R_4=H$ $R_1=CO_2Me$
d. $R_1=R_2=H$ $R_3=CO_2Me$ $R_4=Me$

14

yield:
a-d=quant.

15

yield:
a=55%
b=49%
c=39%
d=72%

Scheme 28. Synthesis of texahydropyrrolinoquinones **15a-d** from tetrahydroquinolines **13a-d**

Along with the synthetic process were detected interesting properties of some compounds. Final compounds **15c-d** shows good fluorescence properties in the free form (**Img. 1**). Detailed studies of a solution of compound **15d** in ACN show high fluorescence at λ=442 nm, log(ε)=3.2 with a quantum yield of 13.0 %, and excitation at λ=320 nm (Stokes shift=122 nm). This property can be useful as a biomolecules' marker, and have potential to be applied in optic coatings, and in food industry.

Img. 1. Solution compound **15d** in DCM, under UV flashlight 325 nm (left), normal light (right)

3.2.4 Addition of 2-(trimethylsililoxy)furan to *p*-methoxy D-erythrosylimine

The crude reaction mixture of the synthesis of imine **16** (lit. [4]) was refrigerated at - 80 °C and BF_3.ether (0.3 eq.) was added, followed by 2-(trimethylsililoxy)furan. The temperature was left to raise till -20 °C for 1 h (**Scheme 7**). The obtained crude showed that the reaction did not followed a Diels-Alder cycloaddition mechanism, but rather a simple nucleophilic addition. Assuming that the facial selectivity of the nucleophilic attack to imine **16** is the same as the observed before for 1-(*tert*-butyldimethylsilyloxy)-1-methoxyethene [12], and for the Diels-Alder cycloadducts [4], the adduct obtained would be *S* configuration at the new stereogenic center in the sugar moiety [13]. The immediate intermediate of the reaction would be structure **17** in equilibrium with **18**. After raising the temperature for 2 h followed by aqueous work-up (a few drops or liquid-liquid extraction) furanone **19** was obtained in *c.a.* 80% yield in 1:1 ratio, according to ^{1}H NMR. When the reaction mixture was transferred after the 2 h time to the freezer for three days, a simple filtration / evaporation, the ratio of isomers was raised to 3 :1. The ratio is maintained when the crude was re-dissolved and submitted to aqueous work-up. The identity of isomers can only be confirmed by crystallography. NMR techniques such as NOESY and COSY are not able to distinguish between isomers due to large number of conformations of these molecules. According to literature [13] the second stereocenter in the molecule (in the furan moiety) can be controlled by the first stereocenter. Other examples in the literature however show a different trend of results. Quenching of a reaction of a D-glyceraldehyde aliphatic imine at -85 °C with water/$NaHCO_3$ led to a 1:1 mixture of diastereomers. The author refer that an isomerization is not excluded during the quenching treatment [14]. A couple of new experiments can shed so light in the reaction in **Scheme 7**: 1) reaction at -80 °C during some time (*e.g.* 5 h) followed by water/$NaHCO_3$ treatment will show the kinetic product, if an isomerization does not occur. [Exclusion of the isomerization during water treatment is based on the 3: 1 ratio of isomers of the reaction kept in the freezer at -20 °C before and after water treatment, against the 1:1 ratio of products obtained with the same protocol after leading the reaction mixture to recover at room temperature, followed by water treatment.] 2) reaction at -80°C during the same time as in 1), followed by reaction mixture temperature rising (say -40 °C for some time). This will give an idea if a thermodynamic equilibrium between **17** and **18** is at work.

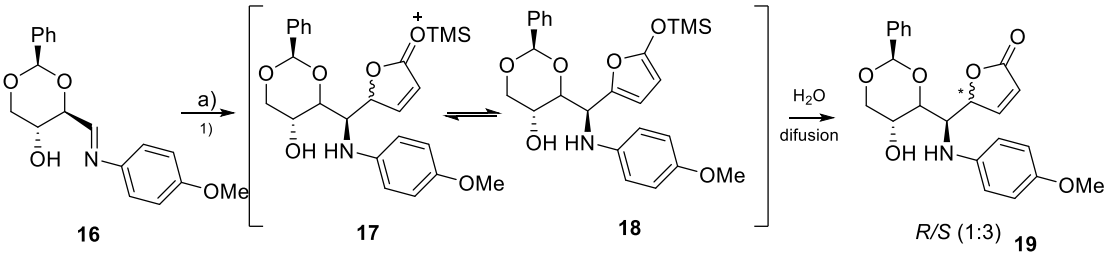

a) 1) THF, -80 to -20 ºC, 2 h., $BF_3.OEt_2$, 2-(trimethylsiloxy)furan (1.1 eq.), N_2(g) 2) -20 ºC, 3 days, yield 82% from **5**

Scheme 7. Nucleophilic addition of the 2-(trimethylsilyloxy)furan to imine **16**

3.3 Conclusions

Method described provide cyclize thiol chain of THQ to HHPQ with good overall yield, that allow synthesize new pool HHPQ compounds from different 4-subsituted THQs. New HHPQ will be biologically evaluated in cancer cell lines. Was conclude that bets way to orientate *m*-substituted group for "top" are using methyl ester which in future could be functionalized *via* transesterification. To guide the ester group to "bottom" position *meta* and *ortho* substituted aniline should be used.

3.4 Experimental section

All reagents were purchased from Sigma-Aldrich, Acros, TCI or Alfa Aesar and used without further purification. THF was dried by reflux under Na(s), ACN by reflux under CaH_2(s). In reactions was used fresh distilled $BF_3.OEt_2$. Aniline purified by stream distillation, liquid-liquid extraction with DCM, and drained with $CaCl_2$. Flash chromatography was performed using silica 60 Å 0.060–0.200 mm, and dry-flash chromatography using silica 60 Å 0.035–0.070 mm as stationary phases.

Synthesis of imines 8a-d

General procedure

To a solution of aldehyde **5** (150-200 mg; 0.72-0.96 mmol, 1.0-1.3 eq.) in dry solvent, containing activated 4 Å molecular sieves was added the anilines (63-110 mg; 0.50-0.67 mmol) under magnetic stirring and N_2 atmosphere. The reaction mixture was kept stirring for 1-3 hours at 35 °C. Reactions were controlled by TLC.

Synthesis of (2*R*,4*S*,5*R*)-2-phenyl-4-((*E*)-(phenylimino)methyl)-1,3-dioxan-5-ol (8a)

Aldehyde **5** (247 mg, 1.19 mmol, 1.1 eq.) Aniline (100 uL; 1.08 mmol) ACN (8 mL), 3 hours.

Synthesis of methyl 3-(((*E*)-((2*R*,4*S*,5*R*)-5-hydroxy-2-phenyl-1,3-dioxan-4-yl)methylene)amino)benzoate (8b)

Aldehyde **5** (100 mg, 0.48 mmol, 1.0 eq.) methyl 3-aminobenzoate (75 mg; 0.48 mmol) THF (4 mL), 1 hour.

Synthesis of ethyl 3-(((*E*)-((2*R*,4*S*,5*R*)-5-hydroxy-2-phenyl-1,3-dioxan-4-yl)methylene)amino)benzoate (8c)

Aldehyde **5** (100 mg, 0.48 mmol, 0.7 eq.) ethyl 3-aminobenzoate (116 mg; 0.70 mmol) THF (4 mL), 2 hours.

Synthesis of isopropyl 3-(((*E*)-((2*R*,4*S*,5*R*)-5-hydroxy-2-phenyl-1,3-dioxan-4-yl)methylene)amino)benzoate (8d)

Aldehyde **5** (281 mg, 1.35 mmol, 0.83 eq.) isopropyl 3-aminobenzoate (290 mg; 1.61 mmol) THF (6 mL), 2 hours.

Synthesis of methyl 3-(((*E*)-((2*R*,4*S*,5*R*)-5-hydroxy-2-phenyl-1,3-dioxan-4-yl)methylene)amino)-2-methylbenzoate (11)

Aldehyde **5** (220 mg, 1.05 mmol, 1.2 eq.) methyl 3-amino-2-methylbenzoate (143 mg; 0.83 mmol) THF (8 mL), 2 hours.

Synthesis of THQs

General procedure

To a recently made imine reaction mixture, maintained under N_2 atmosphere, and cooled to -40 or to -80 °C was added BF_3.etherate (0.3 eq.) followed by *N*-vinyl-pyrrolidone (1.1-5.0 eq.). The mixture was stirred for 10 min at the same temperature after reagents' addition and then allowed to reach room temperature. Reaction time: 2-16 hours. The reaction mixture was filtered through a pad of Celite® washed with DCM or THF, and the solvent evaporated to dryness.

Synthesis of 1-((2*R*,4*R*)-2-((2R,4S,5R)-5-hydroxy-2-phenyl-1,3-dioxan-4-yl)-1,2,3,4-tetrahydroquinolin-4-yl)pyrrolidin-2-one (10a)

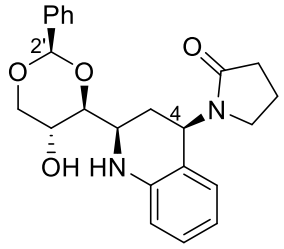

Previous imine **8a** reaction mixture; *N*-vinylpyrrolodione (0.15 mL; 1.5 eq.); time: 16 h. Celite® washed with DCM. The crude residue was dissolved hot ethanol and precipitated with water. The pure product was obtained as a light beige solid (207 mg; η=52%). $[\alpha]_D^{20}$: -63.0 (c=0.01 g/mL in MeOH); FTIR (nujol) ν_{max} 3335; 1653 cm^{-1} m.p.= 126.3-127.8 °C; ^{1}H-NMR (400 MHz, $CDCl_3$): δ_H 1.99-2.07 (m, 3H, *H*-4''+*H*-3), 2.41 (ddd, *J*=12.3 and 5.9; 2.2 Hz, 1H, *H*-3), 2.49-2.54 (m, 2H, *H*-3''), 3.18 (ddd, *J*=9.8 and 7.5; 5.6 Hz, 1H, *H*-5''), 3.28 (dt, *J*=9.8 and 7.5, 1H, *H*-5''), 3.61-3.66 (m, 2H, *H*-6'+*H*-4'), 3.78 (ddd, *J*=12.3 and 5.9; 2.2 Hz, 1H, *H*-5'), 3.92 (td, *J*=9.7 and 5.1 Hz, 1H, *H*-2), 4.28 (dd, *J*=10.9 and 5.3 Hz, 1H, *H*-6'), 5.52 (s, 1H, *H*-2'), 5.56 (dd, *J*=12.2 and 5.9 Hz, 1H, *H*-4), 6.57 (d, *J*=8.2 Hz, 1H, *H*-8), 6.71 (t, *J*=7.4, 1H, *H*-6), 6.82 (d, *J*=7.2 Hz, 1H, *H*-5), 7.01 (d, *J*=7.2 Hz, 1H, *H*-7), 7.38-7.40 (m, 3H, Ph), 7.48-7.51 (m, 2H, Ph) ppm. ^{13}C-NMR (100 MHz, $CDCl_3$): δ_c 18.1 (CH_2, C-4''), 28.3 (CH_2, C-3), 31.4 (CH_2, C-3''), 42.5 (CH_2, C-5''), 48.0 (CH, C-4), 54.0 (CH, C-5'), 63.3 (CH, C-2), 71.1 (CH_2, C-6'), 82.9 (CH, C-4'), 101.1 (CH, C-2'), 116.0 (CH, C-8), 118.6 (CH, C-6), 119.7 (C_q, C-4a), 126.4 (CH, C-5), 128.2 (CH, C-7), 126.2, 128.3, 129.1 (CH, C-Ph), 137.0(C_q, C-Ph) 144.8 (C_q, C-8a), 176.0 (CO) ppm.

Synthesis of methyl (2*R*,4*R*)-2-((2*R*,4*S*,5*R*)-5-hydroxy-2-phenyl-1,3-dioxan-4-yl)-4-(2-oxopyrrolidin-1-yl)-1,2,3,4-tetrahydroquinoline-5-carboxylate (10b)

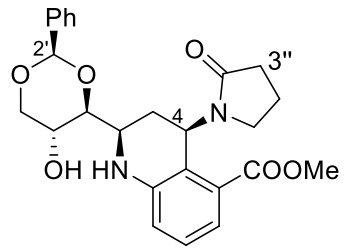

Previous imine **8b** reaction mixture; *N*-vinylpyrrolodione (0.05 mL; 1.1 eq.) time: 4 h. Celite® washed with THF. The crude residue was dissolved in DCM (150 mL) and extracted with aqueous solution of $HNaCO_3$ 10% (50 mL), water (50 mL) and aq. saturated solution NaCl (50 mL). The organic phase dried under $MgSO_4$ anhydrous, the solvent was removed to give a brown foam. The pure product was isolated by flash chromatography (h=15.0 cm Ø=2.0 cm), silica, DMC:EtOH (9.5:0.5). Compound **10b** isolated as transparent oil (94 mg; η=44%). $[\alpha]_D^{20}$: -115.0 (c=0.01 g/mL in MeOH); FTIR (nujol) ν_{max} 3358; 1665 cm^{-1}. ^{1}H-NMR (400 MHz, $CDCl_3$): δ_H 1.82 (q, *J*=12.5 Hz, 1H, *H*-3), 1.83-1.95 (m, 2H, *H*-4''), 2.35 (td, *J*=8.1 and 2.1 Hz, 2H, *H*-3''), 2.57 (ddd, *J*=12.7 and 7.5; 2.1 Hz, 1H, *H*-3), 2.92 (ddd, *J*=9.7 and 7.2; 5.4 Hz, 1H, *H*-5''), 3.09 (dt, *J*=9.5 and 7.6 Hz, 1H, *H*-5''), 3.61-3.69 (m, 2H, *H*-5'+*H*-4'), 3.71 (t, *J*=7.4 Hz, 1H, *H*-6'), 3.75 (s, 3H, OC*H*$_3$), 3.94 (dt, *J*=9.6 and 5.7 Hz, 1H, *H*-2), 4.27 (dd, *J*=11.0 and 5.3 Hz, 1H, *H*-6'), 5.52 (s, 1H, *H*-2'), 5.81 (dd, *J*=11.5 and 7.4 Hz, 1H, *H*-4), 6.68 (dd, *J*=8.2 and 1.3 Hz, 1H, *H*-8), 6.91 (dd, *J*=7.4 and 1.3 Hz, 1H, *H*-6), 7.06 (t, *J*=8.0 Hz, 1H, *H*-7), 7.43-7.36 (m, 3H, Ph), 7.53-7.45 (m, 2H, Ph) ppm. ^{13}C-NMR (100 MHz, $CDCl_3$): δ_c 17.7 (CH_2, C-4''), 28.5 (CH_2, C-3), 31.4 (CH_2, C-3''), 42.5 (CH_2, C-5''), 47.0 (CH, C-4), 52.6 (CH_3, CO_2*Me*), 53.4 (CH, C-5') 63.4 (CH, C-2), 71.2 (CH_2, C-6'), 82.8 (CH, C-4'), 101.1 (CH, C-2'), 117.8 (C_q, C-THQ), 118.9, 119.4 (CH, C-THQ), 126.1(CH, C-Ph), 128.0 (CH, C-THQ), 128.3, 129.1 (CH, C-Ph), 133.1, 137.4, 146.1 (C_q), 170.0 (CO), 175.4 (CO_2Me) ppm.

HRMS(ESI) calcld for $C_{25}H_{29}N_2O_6$ [M+H]: 453.1981; found: 453.2020 *m/z*.

Synthesis of methyl (2*R*,4*R*)-2-((2*R*,4*S*,5*R*)-5-hydroxy-2-phenyl-1,3-dioxan-4-yl)-8-methyl-4-(2-oxopyrrolidin-1-yl)-1,2,3,4-tetrahydroquinoline-7-carboxylate (12)

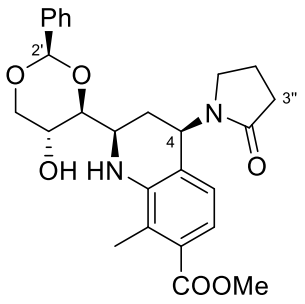

Previous imine **11** reaction mixture; *N*-vinylpyrrolodione (0.6 mL; 5 eq.); time: 16 h. Celite® washed with THF. The crude residue was dissolved in DCM (150 mL) and extracted with aqueous solution of $HNaCO_3$ 10% (50 mL), water (50 mL) and aq. saturated solution NaCl (50 mL). The organic phase dried under $MgSO_4$ anhydrous, the solvent was removed. Product was precipitated using a mixture of ethyl acetate/ petroleum ether to give a white solid (120 mg; η=30%). Θ (degradation)= 195 °C; $[\alpha]_D^{23}$: -36.4 (c=0.01 g/mL in MeOH); FTIR (nujol) ν_{max} 3302; 1650 cm^{-1}; ^{1}H-NMR (400 MHz, $CDCl_3$): δ_H 1.96-2.05 (m, 3H, *H*-3+*H*-4''), 2.24 (s, 3H, *Me*), 2.35 (ddd, *J*=12.4 and 6.0 Hz; 2.3, 1H, *H*-3), 2.48-2.54 (m, 2H, *H*-3''), 3.10 (ddd, *J*=9.8 and 7.9; 5.1 Hz, 1H, *H*-5''), 3.25 (dt, *J*=9.8 and 7.5 Hz, 1H, *H*-5''), 3.63-3.72 (m, 2H, *H*-6'+*H*-4'), 3.76 (td, *J*=5.8 and 2.3 Hz, 1H, *H*-5'), 3.83 (s, 3H, CO_2*Me*), 3.89-3.95 (m, 1H, *H*-2), 4.29 (dd, *J*=10.8 and 5.3 Hz, 1H, *H*-6'), 5.53 (dd, *J*=11.9 and 5.5 Hz, 1H, *H*-4), 5.55 (s, 1H, *H*-2'), 6.72 (d, *J*=8.2 Hz, 1H, *H*-6), 7.12 (d, *J*=8.2, 1H, *H*-5), 7.36-7.40 (m, 3H, Ph), 7.47-7.49 (m, 2H, Ph) ppm. ^{13}C-NMR (100 MHz, $CDCl_3$): δ_c 13.5 (CH_3, *Me*), 18.1 (CH_2, C-4''), 27.9 (CH_2, C-3), 31.3 (CH_2, C-3''), 42.5 (CH_2, C-5''), 48.4 (CH,C-4), 51.9 (CH, C-5'), 53.5 (CH_3, CO_2*Me*), 63.3 (CH, C-2), 71.1 (CH_2, C-6'), 82.9 (CH, C-4'), 100.8 (CH, C-2'), 119.3 (CH, C-5), 122.5 (C_q, C-4a), 123.4 (CH, C-6), 123.9(C_q, Ph), 125.9, 128.3, 129.0 (CH, Ph), 130.4 (C_q, C-8), 137.4 (C_q, C-7), 143.6 (C_q, C-8a), 168.8 (*C*O), 176.3 (CO_2Me) ppm.

Synthesis of ethyl (2*R*,4*R*)-2-((2*R*,4*S*,5*R*)-5-hydroxy-2-phenyl-1,3-dioxan-4-yl)-4-(2-oxopyrrolidin-1-yl)-1,2,3,4-tetrahydroquinoline-7-carboxylate (9c) and ethyl (2*R*,4*R*)-2-((2*R*,4*S*,5*R*)-5-hydroxy-2-phenyl-1,3-dioxan-4-yl)-4-(2-oxopyrrolidin-1-yl)-1,2,3,4-tetrahydroquinoline-5-carboxylate (10c)

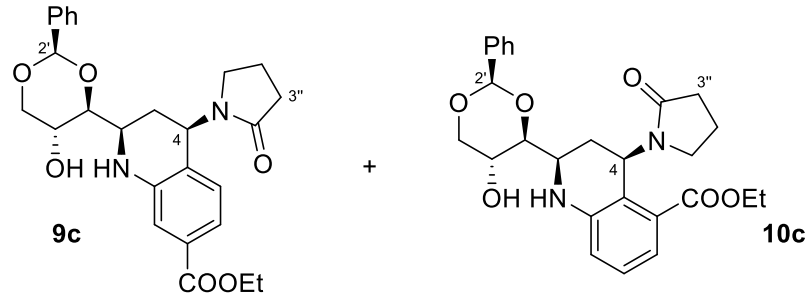

0.7 : **1**

Previous imine **8c** reaction mixture; *N*-vinylpyrrolodione (0.05 mL; 1.1 eq.); time: 2 h. Celite® washed with THF. The crude residue was dissolved in DCM (150 mL) and washed with an 10% aqueous solution of $HNaCO_3$ (50 mL), water (50 mL) and aq. saturated solution NaCl (50 mL). The organic phase was dried under $MgSO_4$ anhydrous, the solvent was removed to give a brown foam. The product was isolated as mixture of diastereomers, as a transparent oil (123 mg; 0.25 mmol; isomeric ratio 0.7:1.0; η=55%) after flash chromatography (h=18.0 cm Ø=0.5 cm), silica, DMC:EtOH (9.5:0.5).

Distinguishable signals: **10c** ^{1}H-NMR (400 MHz, $CDCl_3$): δ_H 1.33 (t, *J*=7.0 Hz, 3H, C*H*$_3$-Et), 2.34 (t, *J*=8.0 Hz, 2H, *H*-3''), 2.90-2.96 (m, 1H, *H*-5''), 3.06-3.12 (m, 1H, *H*-5''), 5.50 (s, 1H, *H*-2'), 5.81 (dd, *J*=11.1 and 7.3 Hz, 1H, *H*-4), 6.69 (d, *J*=8.0 Hz, 1H, *H*-8), 6.90 (d, *J*=7.7 Hz, 1H, *H*-6), 7.06 (t, *J*=7.9 Hz, 1H, *H*-7) ppm. ^{13}C-NMR (100 MHz, $CDCl_3$): δ_c 13.9 (CH_3, C-Et), 31.4 (CH_2, C-3''), 42.6 (CH_2, C-5''), 46.9 (CH, H-4), 101.2 (CH, C-2') ppm.

Distinguishable signals: **9c** ^{1}H-NMR (400 MHz, $CDCl_3$): δ_H 1.33 (t, *J*=7.0 Hz, 3H, C*H*$_3$-Et), 2.51 (t, *J*=8.0 Hz, 2H, *H*-3''), 3.12-3.17 (m, 1H, *H*-5''), 3.29 (dt, *J*=9.5 and 7.5 Hz, 1H, *H*-5''), 5.53 (s, 1H, *H*-2'), 5.57 (dd, *J*=12.4 and 5.7 Hz, 1H, *H*-4), 6.86 (d, *J*=7.9 Hz, 1H, *H*-5), 7.23 (d, *J*=2.0 Hz, 1H, *H*-8), 7.06 (dd, *J*=8.0 and 2.0 Hz, 1H, *H*-6) ppm. ^{13}C-NMR (100 MHz, $CDCl_3$): δ_c 13.9 (CH_3, C-Et), 31.4 (CH_2, C-3''), 42.6 (CH_2, C-5''), 48.2 (CH, H-4), 101.2 (CH, C-2') ppm.

Synthesis of isopropyl (2*R*,4*R*)-2-((2*R*,4*S*,5*R*)-5-hydroxy-2-phenyl-1,3-dioxan-4-yl)-4-(2-oxopyrrolidin-1-yl)-1,2,3,4-tetrahydroquinoline-5-carboxylate (9d) and of isopropyl (2*R*,4*R*)-2-((2*R*,4*S*,5*R*)-5-hydroxy-2-phenyl-1,3-dioxan-4-yl)-4-(2-oxopyrrolidin-1-yl)-1,2,3,4-tetrahydroquinoline-7-carboxylate (10d)

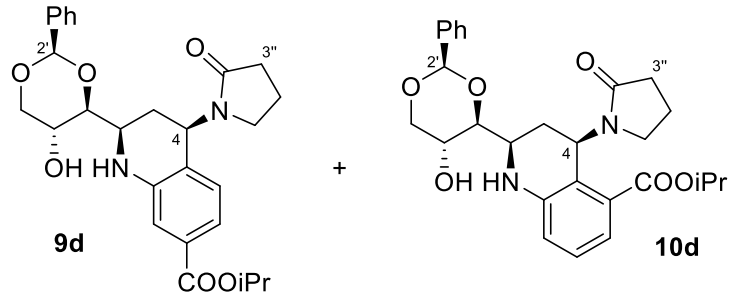

0.4 : **1**

Previous imine **8d** reaction mixture; *N*-vinylpyrrolodione (0.05 mL; 1.1 eq.); time: 3 h. Celite® washed with THF. The crude residue was dissolved in DCM (150 mL) and washed with 10% aqueous $HNaCO_3$ solution (50 mL), water (50 mL) and NaCl aq. saturated solution (50 mL). The organic phase dried under $MgSO_4$ anhydrous, the solvent was removed. Product, consisting of a mixture of isomers was precipitated with ethanol/water giving an amorphous white solid (263 mg; 0.74 mmol; isomeric ratio 0.4:1.0; η=51%).

Distinguishable signals: **10d** ^{1}H-NMR (400 MHz, $CDCl_3$): δ_H 1.30 (d, *J*=6.4 Hz, 6H, C*H*$_3$-*i*Pr), 2.31 (t, *J*=8.2 Hz, 2H, *H*-3''), 2.90-2.94 (m, 1H, *H*-5''), 3.03-3.09 (m, 1H, *H*-5''), 3.57-3.67 (m, 1H, *H*-6'), 4.21 (dd, *J*=10.8 and 5.4 Hz, 1H, *H*-6'), 4.99 (hept, *J*=6.4 Hz, 1H, C*H*-*i*Pr), 5.49 (s, 1H, *H*-2'), 5.51-5.56 (m, 1H, *H*-4), 6.65 (d, *J*=7.9 Hz, 1H, *H*-8), 6.82 (d, *J*=7.7 Hz, 1H, *H*-6), 7.01 (t, *J*=7.8 Hz, 1H, *H*-7) ppm. ^{13}C-NMR (100 MHz, $CDCl_3$): δ_C 21.7 (CH_3, C-*i*Pr), 31.2 (CH_2, C-3''), 42.4 (CH_2, C-5''), 69.2 (CH, C-*i*Pr), 71.1 (CH_2, C-6'), 100.9 (CH, C-2') ppm.

Distinguishable signals: **9d** ^{1}H-NMR (400 MHz, $CDCl_3$): δ_H 1.34 (d, *J*=6.4 Hz, 6H, C*H*$_3$-*i*Pr), 2.38 (m, 2H, *H*-3''), 3.09-3.13 (m, 1H, *H*-5''), 3.25-3.27 (m, 1H, *H*-5''), 3.57-3.67 (m, 1H, *H*-6'), 4.28 (dd, *J*=11.0 and 5.6 Hz, 1H, *H*-6'), 5.12-5.20 (m, 1H, C*H*-*i*Pr), 5.51 (s, 1H, *H*-2'), 5.82 (dd, *J*=10.7 and 7.6 Hz, 1H, *H*-4), 6.82 (d, *J*=8.2 Hz, 1H, *H*-5), 7.20 (d, *J*=2.0 Hz, 1H, *H*-6), 7.29 (dd, *J*=8.0 and 2.0 Hz, 1H, *H*-8) ppm. ^{13}C-NMR (100 MHz, $CDCl_3$): δ_C 21.4 (CH_3, C-*i*Pr), 31.6 (CH_2, C-3''), 42.4 (CH_2, C-5''), 68.1 (CH, C-*i*Pr), 71.1 (CH_2, C-6'), 100.9 (CH, C-2') ppm.

General procedure for acetal cleavage in compounds 10a,b and 12

To a solution of compound **12**, **10a,b** in 1,4-dioxane or THF was added HCl (2 M, 1 mL). and the mixture stirring at r.t. or 35 °C for 19 h and then evaporated to dryness at 65 °C.

Synthesis of 1-((2*R*,4*R*)-2-((1*S*,2*R*)-1,2,3-trihydroxypropyl)-1,2,3,4-tetrahydroquinolin-4-yl)pyrrolidin-2-one hydrochloride (14a)

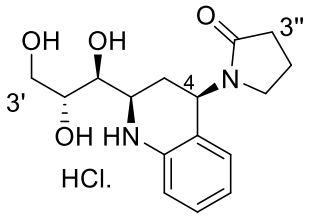

Compound **10a** (100 mg; 0.25 mmol); THF (4 mL), r.t. Product: dark green oil η=quantitative. $[\alpha]_D^{17}$: +11.5 (c=0.01 g/mL in MeOH); FTIR (nujol) ν_{max} 3343; 1666; cm^{-1}. ^{1}H-NMR (400 MHz, D_2O): δ_H 1.95-2.02 (m, 2H, *H*-4''), 2.16-2.26 (m, 2H, *H*-3), 2.48 (t, *J*=8.0 Hz, 2H, *H*-3''), 3.04 (td, *J*=9.4 and 9.0; 4.9 Hz, 1H, *H*-5''), 3.31-3.37 (m, 1H, *H*-5''), 3.61 (dd, *J*=11.7 and 4.6 Hz, 1H, *H*-3'), 3.73-3.77 (m, 1H, *H*-3'), 3.81 (br s, 2H, *H*-1'+*H*-2'), 4.00 (d, *J*=11.5 Hz, 1H, *H*-2), 5.54 (dd, *J*=11.4 and 6.7 Hz, 1H, *H*-4), 7.14-7.17; 7.28-7.30; 7.36-7.38 (m, 4H, *Ar-THQ*) ppm. ^{13}C-NMR (100 MHz, D_2O): δ_c 17.0 (CH_2, C-4''), 25.9 (CH_2, C-3), 30.6 (CH_2, C-3''), 43.1 (CH_2, C-5''), 47.6 (CH, C-4), 55.0 (CH, C-2), 61.8 (CH_2, C-3'), 70.0 ; 70.9 (CH, C-1' or C-2'), 127.3, 127.6, 128.6, 128.8 (CH, Ar-THQ), 122.6 (C_q, C-4a), 131.1 (C_q, C-8a), 179.0 (C_q, CO) ppm.

Synthesis of methyl (2*R*,4*R*)-4-(2-oxopyrrolidin-1-yl)-2-((1*S*,2*R*)-1,2,3-trihydroxypropyl)-1,2,3,4-tetrahydroquinoline-5-carboxylate hydrochloride (14c)

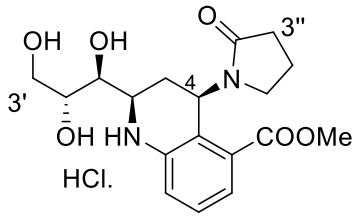

Compound **10b** (100 mg; 0.22 mmol); THF (4 mL); r.t. Product: brown oil; η=quantitative. $[\alpha]_D^{18}$: -25.4 (C=0.01 g/mL in MeOH); FTIR (nujol) ν_{max} 3333; 1665; 1293 cm^{-1}. ^{1}H-NMR (400 MHz, D_2O): δ_H 1.84-2.17 (m, 4H, *H*-3+*H*-4''), 2.42-2.49 (m, 2H, *H*-3''), 2.83 (td, *J*=9.3 and 3.7

Hz, 1H, *H*-5''), 3.25 (dt, *J*=9.8 and 7.9 Hz, 1H, *H*-5''), 3.69-3.76 (m, 2H, *H*-2'+*H*-3'), 3.79 (s, 3H, CO_2*Me*), 3.83-3.90 (m, 3H, *H*-3'+*H*-1'+*H*-2), 5.66 (dd, *J*=11.2 and 7.8 Hz, 1H, *H*-4), 6.97 (dd, *J*=7.3 and 1.2 Hz, 1H, *H*-6 or *H*-8), 6.99 (dd, *J*=8.0 and 1.2 Hz, 1H, *H*-6 or *H*-8), 7.23 (t, *J*=8.0 Hz, 1H, *H*-7) ppm. ^{13}C-NMR (100 MHz, D_2O): δ_c 17.2 (CH_2, C-4''), 27.8 (CH_2, C-3), 31.4 (CH_2, C-3''), 42.7 (CH_2, C-5''), 47.2 (CH, C-4), 51.3 (CH, C-2), 53.3 (CH_3, CO_2Me), 62.6 (CH_2, C-3'), 71.6 (CH_2, C-1'), 82.8 (CH, C-2'), 117.3 (C_q, C-5), 119.7, 120.1 (CH, C-6+C-8), 128.7 (CH, C-7), 132.0 (C_q, C-4a), 146.7 (C_q, C-8a), 172.0 (C_q, CO_2Me), 178.1 (CO) ppm.

Synthesis of methyl (2*R*,4*R*)-8-methyl-4-(2-oxopyrrolidin-1-yl)-2-((1*S*,2*R*)-1,2,3-trihydroxypropyl)-1,2,3,4-tetrahydroquinoline-7-carboxylate hydrochloride salt (14d)

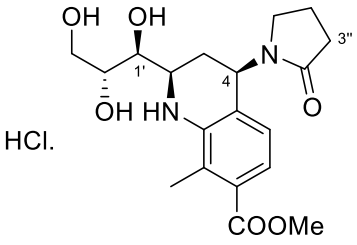

Compound **13d** (100 mg; 0.38 mmol); THF (4 mL); 35 °C. Product: brown oil (142 mg 0.38mmol), η=quantitative. $[\alpha]_D^{23}$: +18.3 (c=0.01 g/mL in MeOH); FTIR (nujol) ν_{max} 3365; 1717; 1652 cm^{-1}. ^{1}H-NMR (400 MHz, D_2O): δ_H 2.01-2.09 (m, 2H, *H*-4'') 2.21-2.35 (m, 2H, *H*-3), 2.40 (s, 3H, *Me*), 2.55 (t, *J*=7.7 Hz, 2H, *H*-3''), 3.05 (br s, 1H, *H*-5''), 3.37-3.43 (m, 1H, *H*-5''), 3.71 (dd, *J*=11.8 and 5.6 Hz, 1H, *H*-3'), 3.81 (dd, *J*=11.8 and 4.8 Hz, 1H, *H*-3'), 3.90 (s, 3H, CO_2*Me*), 3.97-4.02 (m, 3H, *H*-2+*H*-2'+*H*-1'), 5.51 (dd, *J*=11.2 and 6.7 Hz, 1H, *H*-4), 7.09 (d, *J*=8.3, 1H, *H*-6), 7.67 (d, *J*=8.2 Hz, 1H, *H*-5) ppm. ^{13}C-NMR (100 MHz, D_2O): δ_c 13.1 (CH_3, Me), 17.0 (CH_2, C-4''), 25.5 (CH_2, C-3), 30.6 (CH_2, C-3''), 43.1 (CH_2, C-5''), 47.6 (CH, C-4), 52.5 (CH, CO_2*Me*), 55.3 (CH, C-2), 61.2 (CH_2, C-3'), 70.2 (CH, C-1'), 72.8 (CH, C-2'), 124.8 (CH, C-6), 128.0 (CH, C-5), 130.5, 130.9 (C_q, C-7, C-8), 131.1 (C_q, C-4a), 132.9 (C_q, C-8a), 169.0 (C_q, CO_2Me), 178.8 (C_q, CO) ppm.

Synthesis of methyl (2*R*,3*S*,3a*R*,5*R*)-2,3-dihydroxy-5-(2-oxopyrrolidin-1-yl)-1,2,3,3a,4,5-hexahydropyrrolo[1,2-*a*]quinoline-6-carboxylate (15c)

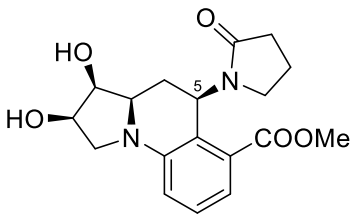

Compound **14c** (104 mg; 0.26 mmol) was solubilized in glacial acetic acid (0.5 mL) and HBr in acetic acid 33% (0.5 mL) was added, and leaved stirring for 1 hour at 25 °C. MeOH (15 mL) was added and mixture stirred for 19 h at 25 °C. Another portion of MeOH (15 mL) was added followed by solid Na_2CO_3 (0.5 g) and water (0.5 mL) slowly addition. The mixture was stirred for 3 hours at 25 °C then evaporated to dryness, to give a crude solid, which was washed with THF, filtered and the solution evaporated. Final compound was deposited as brown oil in mixture DCM/hexane with (35 mg 0.10 mmol) η=39%. $[\alpha]_D^{25}$: -84.3 (c=0.01 g/mL in MeOH); ^{1}H-NMR (400 MHz, $CDCl_3$): δ_H 1.86-2.13 (m, 4H, *H*-4'+*H*-4), 2.29-2.38 (m, 2H, *H*-3') 2.92 (ddd, *J*=9.7 and 8.0; 4.5 Hz, 1H, *H*-5'), 3.09 (dt, *J*=9.8 and 7.7 Hz, 1H, *H*-5'), 3.24 (dd, *J*=9.6 and 6.3 Hz, 1H, *H*-1), 3.46-3.50 (m, 1H, *H*-1), 3.54 (br d, 1H, *H*-3a), 3.74 (s, 3H, CO_2*Me*), 4.17 (br s, 1H, *H*-2), 4.49 (br s, 1H, *H*-3), 5.77 (dd, *J*=11.6 and 7.3 Hz, 1H, *H*-5), 6.51 (dd, *J*=8.3 and 1.3 Hz, 1H, *H*-7), 6.80 (dd, *J*=7.5 and 1.1 Hz, 1H, *H*-9), 7.13 (t, *J*=7.9 Hz, 1H, *H*-8) ppm. ^{13}C-NMR (100 MHz, $CDCl_3$): δ_c 17.2 (CH_2, C-4'), 25.2 (CH_2, C-4), 31.5 (CH_2, C-3'), 42.6 (CH_2, C-5'), 47.3 (CH, C-5), 52.0 (CH_2, C-1), 52.6 (CH_3, CO_2*Me*), 58.4 (CH, C-3a), 70.8 (CH, C-3), 72.5 (CH, C-2), 114.1 (CH, C-7), 116.8 (CH, C-9), 116.9(C_q, C-6) 128.5 (CH, C-8), 132.9 (C_q, C-5a), 145.7 (C_q, C-9a), 170.4 (C_q, CO_2Me), 175.5 (C_q, CO) ppm.

Synthesis of methyl (2*R*,3*S*,3a*R*,5*R*)-2,3-dihydroxy-9-methyl-5-(2-oxopyrrolidin-1-yl)-1,2,3,3a,4,5-hexahydropyrrolo[1,2-*a*]quinoline-8-carboxylate (15d)

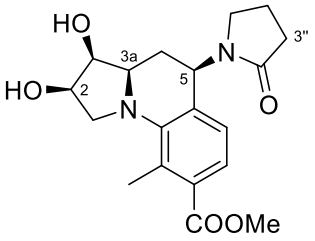

Compound **14d** (28 mg; 0.067 mmol) was solubilized in HBr in acetic acid 33% (1 mL), and leaved stirring for 2 hours at 25 °C. MeOH (5 mL) was added and mixture stirred for 19 h at 25 °C. Another portion of MeOH (15 mL) was added followed by solid Na_2CO_3 (0.5 g) and water (0.5 mL) slowly addition. The mixture was stirred for 3 hours at 25 °C then evaporated to dryness, to give a crude solid, which was washed with THF, filtered and the solution evaporated. Final compound was deposited as brown oil in mixture DCM/hexane with (17.5 mg; 0.49 mmol) η=72%. $[\alpha]_D^{27}$: -26.0 (c=0.01 g/mL in MeOH); ^{1}H-NMR (400 MHz, $CDCl_3$): δ_H 1.85 (ddd, *J*=12.5; 6.7 and 2.3 Hz, 1H, *H*-4), 1.98-2.07 (m, 3H, *H*-4'+*H*-4), 2.35 (s, 3H, *Me*), 2.48-2.54 (m, 2H, *H*-3'), 2.86 (dd, *J*=10.9 and 2.9 Hz, 1H, *H*-1), 3.07 (ddd, *J*=9.8; 7.9 and 5.1 Hz, 1H, *H*-5'), 3.25 (dt, *J*=9.9 and 7.5 Hz, 1H, *H*-5'), 3.68-3.74 (m, 1H, *H*-3a), 3.87 (s, 3H, CO_2*Me*), 3.93 (dd, *J*=11.1 and 5.7 Hz, 1H, *H*-1), 4.34-4.42 (m, 2H, *H*-2 + *H*-3), 5.52 (dd, *J*=12.1 and 6.6 Hz, 1H, *H*-5), 6.82 (d, *J*=8.2 Hz, 1H, *H*-7), 7.35(d, *J*=8.2 Hz, 1H, *H*-6) ppm. ^{13}C-NMR (100 MHz, $CDCl_3$): δ_c 17.4 (CH_3, Me), 18.0 (CH_2, C-4'), 21.8 (CH_2, C-4), 31.4 (CH_2, C-3'), 42.6 (CH_2, C-5'), 49.6 (CH, C-5), 52.0 (CH_3, CO_2*Me*), 58.3 (CH_2, C-1), 60.1 (CH, C-3a), 70.6 (CH, C-3), 71.1 (CH, C-2), 122.8 (CH, C-6), 123.7 (CH, C-7), 129.0 (C_q, C-5a), 131.4 and 131.6 (C_q, C-8 and C-9), 147.5 (C_q, C-9a), 168.8 (C_q, CO_2Me), 176.2 (CO) ppm.

Synthesis of 1-((2*R*,3*S*,3a*R*,5*R*)-2,3-dihydroxy-1,2,3,3a,4,5-hexahydropyrrolo[1,2-*a*]quinolin-5-yl)pyrrolidin-2-one (15a)

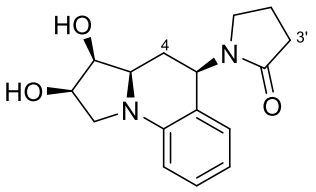

Crude mixture of **14a** (0.15mmol) was solubilized in glacial acetic acid (3 mL) and HBr in acetic acid 33% (0.5 mL) was added, the mixture leaved at stirring for 1 hours at 25 °C. MeOH (20 mL) was added and mixture stirred for 19 h at 25 °C. Followed by solid Na_2CO_3 (0.5 g) was added and water (0.5 mL). The mixture was stirred for 2 hours at 40 °C then evaporated to dryness, to give a crude solid, which submitted flash chromatography followed by gradient elution (DCM to DCM/EtOH/NH_3 (aq 25%) 10:1:0.1) (24 mg 0.08 mmol) η=55%. $[\alpha]_D^{22}$: -16.3 (c=0.01 g/mL in MeOH); ^{1}H-NMR (400 MHz, $CDCl_3$): δ_H 1.93-2.17 (m, 4H, *H*-4'+*H*-4), 2.49-2.55 (m, 2H, *H*-3'), 3.15 (dd, *J*=9.3 and 7.0 Hz, 1H, *H*-1), 3.21 (t, *J*=6.5 Hz, 1H, *H*-5'), 3.25-3.31 (m, 1H, *H*-5'), 3.52 (t, *J*=8.8 Hz, 1H, *H*-1), 3.68 (dt, *J*=11.3 and 3.3 Hz, 1H, *H*-3a), 4.11 (t, *J*=3.9 Hz, 1H, *H*-2), 4.51 (td, *J*=7.6 and 4.3 Hz, 1H, *H*-3), 5.53 (dd, *J*=12.2 and 5.5 Hz, 1H, *H*-5), 6.38 (d, *J*=8.0 Hz, 1H, *H*-9), 6.61 (t, *J*=7.4 Hz, 1H, *H*-7), 6.77 (d, *J*=7.6, 1H, *H*-6), 7.10 (t, *J*=8.0 Hz, 1H, *H*-8) ppm. ^{13}C-NMR (100 MHz, $CDCl_3$): δ_c 18.2 (CH_2, C-4'), 25.0 (CH_2, C-4), 31.5 (CH_2, C-3'), 42.5 (CH_2, C-5'), 48.2 (CH, C-5), 51.6 (CH_2, C-1), 59.4 (CH, C-3a), 71.0 (CH, C-3), 72.7 (CH, C-2), 111.1 (CH, C-9), 116.0 (CH, C-7), 118.4 (C_q, C-5a), 125.7 (CH, C-6), 128.5 (CH, C-8), 144.7 (C_q, C-9a), 176.1 (CO) ppm.

Synthesis 1-((2*R*,3*S*,3*aR*,5*R*)-2,3-dihydroxy-7-methoxy-1,2,3,3a,4,5-hexahydrobenzo-[*e*]indolizin-5-yl)pyrrolidin-2-one (15b)

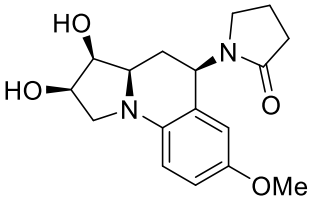

Crude mixture of **14b** (105 mg; 0.28 mmol) was solubilized in HBr in acetic acid 33% (1.5 mL), the mixture leaved at stirring for 1 hours at 25 °C. MeOH (10 mL) was added and mixture stirred for 19 h at 25 °C. Followed was added $HNaCO_3$ (0.5 g) and water (1 mL). The mixture was stirred for 19 hours at 25 °C then evaporated to dryness, to give a crude solid, which dissolved in DCM and precipitated with *n*-hexane as gray precipitate. Precipitate was filtered and removed from filter paper by washing with DCM, solvent removed to give brown oil (48 mg; 0.138 mmol) η=49%. $[\alpha]_D^{21}$: -19.3 (c=0.01 g/mL in MeOH); FTIR (nujol) ν_{max} 3495; 3190; 1665 cm^{-1}. ^{1}H-NMR* (400 MHz, $CDCl_3$): δ_H 1.98-2.07 (m, 3H, *H*-4'+*H*-4), 2.13 (q, *J*=12.0 Hz, 1H, *H*-4), 2.49-2.54 (m, 2H, *H*-3'), 3.16-3.23 (m, 2H, *H*-1+*H*-5'), 3.26-3.30 (m, 1H, *H*-5'), 3.42 (t, *J*=8.4 Hz, 1H, *H*-1), 3.56 (dt, *J*=12.0 and 2.4 Hz, 1H, *H*-3a), 3.70 (s, 3H, O*Me*), 4.11 (t, *J*=4.0 Hz, 1H, *H*-2), 4.50 (dd, *J*=12.3 and 6.5 Hz, 1H, *H*-3), 5.53 (dd, *J*=12.3 and 6.0 Hz, 1H, *H*-5), 6.35 (d, *J*=8.8 Hz, 1H, *H*-9), 6.43 (dd, *J*=2.4 and 0.8 Hz, 1H, *H*-6), 6.71 (dd, *J*=8.7 and 2.8 Hz, 1H, *H*-8) ppm. ^{13}C-NMR** (100 MHz, $CDCl_3$): δ_c 18.2 (CH_2, C-4'), 25.3 (CH_2, C-4), 31.4 (CH_2, C-3'), 42.4 (CH_2, C-5'), 48.3 (CH, C-5), 52.5 (CH_2, C-1), 55.9 (OMe), 59.8 (CH, C-3a), 70.8 (CH, C-3), 72.5 (CH, C-2), 111.9 (CH, C-9), 112.6 (CH, C-6), 118.4, (C_q, C-5a), 113.4 (CH, C-8), 120.2 (C_q, C-5a), 151.1 (C_q, C-7), 175.8 (CO) ppm.

*spectra record with D1=3.0 s if D1=1.0 s spectra will contain two rotamers.

**contaminated with triethylammonium salt.

HRMS(ESI) calcld for $C_{17}H_{21}N_2O_4$ [M-H]: 317.1507; found: 317.1501 *m/z*.

Synthesis of 5-((1*R*)-((2*R*,5*R*)-5-hydroxy-2-phenyl-1,3-dioxan-4-yl)((4-methoxyphenyl)-amino)methyl)furan-2(5*H*)-one (19)

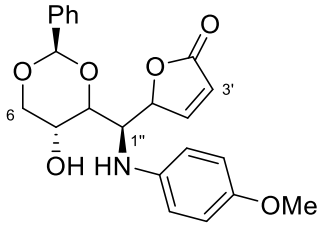

The imine (0.50 mmol) reaction solution in dry THF (4 mL) was prepared according with literature [4], refrigerated till -80 °C, and kept stirring under nitrogen atmosphere. BF_3.ether (0.3 eq.) was added first followed by 2-(trimethylsililoxy)furan (100 μL, 1.2 eq.) The mixture was stirred for 1.5 h with allowing rise temperature. The temperature rose till -20 °C and the reaction flask was transferred to the freezer (-20 °C) for 3 days. Mixture was filtered, the solvent evaporated, giving a dark brown oil. This oil was re-dissolved in DCM (100 mL) and washed with water (3 x 50 mL). Organic phase was dried over $MgSO_4$. The solvent was evaporated to give a brown oil showed to be a 3:1 mixture of isomers (162 mg, 0.41 mmol) η=82%.

Major diastereomer (distinguishable signals)

^{1}H-NMR (400 MHz, $CDCl_3$): δ_H 3.61 (t, *J*=10.5 Hz, 1H, *H*-6), 3.74 (s, 3H, O*Me*), 4.13-4.14 (m, 1H, H-5), 4.25 (dd, *J*=10.8 and 5.8 Hz, 1H, *H*-6), 5.19 (dt, *J*=10.8 and 5.8 Hz, 1H, H-5'). 5.60 (s, 1H, *H*-2), 6.12 (dd, *J*=5.7 and 2.0 Hz, 1H, *H*-3'), 6-54-6.58 and 6-71-6.82 (m, 4H, *Ar*-OMe), 7.39-7.45 (m, 3H, Ph), 7.49-7.51 (m, 2H, Ph) ppm. ^{13}C-NMR (100 MHz, $CDCl_3$): δ_c 55.6 (CH_3, OMe), 71.0 (CH_2, C-6), 80.8 (CH, C-5), 82.2 (CH, C-5'), 100.9 (CH, C-2), 156.5 (CH, C-4'), 172.9 (C_q, CO) ppm.

* The signal of H-4' is shown separately in the ^{1}H-NMR spectrum taken in CD_3OD: 7.59 (dd, *J*=5.8 and 2.0 Hz, 1H, H-4') ppm.

Minor diastereomer (distinguishable signals)

^{1}H-NMR (400 MHz, $CDCl_3$): δ_H 3.61 (dd, *J*=10.0 and 10.8 Hz, 1H, *H*-6), 3.74 (s, 3H, O*Me*), 3.77-3.79 (m, 1H, H-1''), 4.33 (dd, *J*=11.0 and 5.6 Hz, 1H, *H*-6), 5.36 (dt, *J*=5.2 and1.9 Hz, 1H, H-5'), 5.44 (s, 1H, *H*-2), 6.07 (dd, *J*=5.7 and 2.0 Hz, 1H, *H*-3'), 6-54-6.58 and 6-71-6.82 (m, 4H, *Ar*-OMe), 7.39-7.45 (m, 3H, Ph), 7.49-7.51 (m, 2H, Ph) ppm. ^{13}C-NMR (100 MHz, $CDCl_3$): δ_c 55.6

(CH_3, OMe), 71.0 (CH_2, C-6), 80.8 (CH, C-5), 82.2 (CH, C-5'), 101.3 (CH, C-2), 156.5 (CH, C-4'), 172.9 (C_q, CO) ppm.

* The signal of H-4' is shown separately in the ^{1}H-NMR spectrum taken in CD_3OD: 7.71 (dd, J=5.8 and 2.0 Hz, 1H, H-4') ppm.

Supporting Information (NMR Data) available at attached file.

3.5 References

(1) Sridharan, V.; Suryavanshi, P. A.; Menéndez, J. C. Advances in the Chemistry of Tetrahydroquinolines. *Chem. Rev.* **2011**, *111* (11), 7157–7259. https://doi.org/10.1021/cr100307m.

(2) Muthukrishnan, I.; Sridharan, V.; Menéndez, J. C. Progress in the Chemistry of Tetrahydroquinolines. *Chem. Rev.* **2019**, *119* (8), 5057–5191. https://doi.org/10.1021/acs.chemrev.8b00567.

(3) World Health Organization. WHO Model Formation. 2009, p 96.

(4) Ferreira, J.; Duarte, V. C. M.; Noro, J.; Gil Fortes, A.; Alves, M. J. Total Facial Selectivity of a D-Erythrosyl Aromatic Imine in [4π + 2π] Cycloadditions; Synthesis of 2-Alkylpolyol 1,2,3,4-Tetrahydroquinolines. *Org. Biomol. Chem.* **2016**, *14* (10), 2930–2937. https://doi.org/10.1039/c5ob02594j.

(5) Baker, S. R.; Clissold, D. W.; McKillop, A. Synthesis of Leukotriene A4 Methyl Ester from D-Glucose. *Tetrahedron Lett.* **1988**, *29* (9), 991–994. https://doi.org/10.1016/0040-4039(88)85316-4.

(6) Schmidt, R. R.; Zimmermann, P. Synthesis of D-Erythro-Sphingosines. *Tetrahedron Lett.* **1986**, *27* (4), 481–484. https://doi.org/10.1002/jlac.198819880708.

(7) Zimmermann, P.; Schmidt, R. R. Synthese von Erythro-Sphingosinen Über Die Azidoderivate. *Liebigs Ann. der Chemie* **1988**, No. 7, 663–667. https://doi.org/10.1016/S0040-4039(00)85510-0.

(8) Fengler-Veith, M.; Schwardt, O.; Kautz, U.; Krämer, B.; Jäger, V. (1′R)-(−)-2,4-O-Ethylidene- D -Erythrose and Ethyl (E)-(−)-4,6-O-Ethylidene-(4S,5R,1′R)-4,5,6-Trihydroxy-2-Hexenoate. *Org. Synth.* **2002**, *78* (September), 123. https://doi.org/10.15227/orgsyn.078.0123.

(9) Freitas, D. S.; Sousa, C.; Parente, J.; Drogalin, A.; Fortes, A. G.; Cerqueira, N.; Alves, M. J. A Two Step Synthesis of (3S,4R)-Dihydroxy-N-Alkyl L-Homoprolines from D-Erythrose. Computational Mechanistic Studies. *Org. Biomol. Chem.* **2019**, submitted.

(10) Li, J.; Sha, Y. A Convenient Synthesis of Amino Acid Methyl Esters. *Molecules* **2008**, *13* (5), 1111–1119. https://doi.org/10.3390/molecules13051111.

(11) Pearson, A. J.; Roush, W. R. *Handbook of Reagents for Organic Synthesis, Activating Agents and Protective Groups*, John Wiley.; 1999.

(12) Freitas, D. S.; Sousa, C. E. A.; Parente, J.; Drogalin, A.; Fortes, A. G.; Cerqueira, N. M. S. F. A.; Alves, M. J. A Two Step Synthesis of (3S,4R)-Dihydroxy-N-Alkyl L-Homoprolines from D-Erythrose. Computational Mechanistic Studies. *Org. Biomol. Chem.* **2019**, [accepted].

(13) Spanedda, M. V.; Ourévitch, M.; Crousse, B.; Bégué, J. P.; Bonnet-Delpon, D. Vinylogous Mannich Reactions. Additions of Trimethylsilyloxyfuran to Fluorinated Aldimines. *Tetrahedron Lett.* **2004**, *45* (26), 5023–5025.

https://doi.org/10.1016/j.tetlet.2004.05.003.

(14) Rassu, G.; Pinna, L.; Spanu, P.; Culeddu, N.; Casiraghi, G. Total Synthesis of 1,5-Dideoxy-1,5-Iminoalditols. *Tetrahedron* **1992**, *48* (4), 727–742. https://doi.org/10.1016/S0040-4020(01)88132-1.

Chapter IV: Final conclusions

“I’m conclude that when I’m done with

my thesis, life will be better.”

Internet meme.

4.1 Conclusions and future perspectives

New methodology of synthesis for novel HHPQs was successfully implemented, with moderate yields, through aminocyclization of functionalized THQ. This synthetic pathway could be useful for synthesis of new pool of compounds with improved biological characteristics. The compounds obtained will be biologically evaluated and followed by theoretical studies to understand better the systems and the process involved in inhibition of mannosidases.

Theoretical work helped to find out two new perspective HHPQs compounds having affinity towards human model of Golgi α-mannosidase II. These molecules possess a viable synthetic route.

The computational procedure implemented in this works serves also to optimize the theoretical calculation protocol, as the perception about the most suitable and efficient method to treat this type of system.

As future perspectives, the synthesis of the novel HHPQs suggested by molecular modelling will be addressed, followed by their biological evaluation. Also, the four synthesized molecules will be evaluated with the same computational protocol here implemented, as well as will be biologically tested.

The complementarity of these methods allows a more rational design of active compounds, saving time and resources. In this process, important aspects behind an optimum binding and activity are disclosed, from different techniques and point of views.

The End